

THE ADSORPTION OF RADIOACTIVE ISOTOPES  
ON SPECIFIC PRECIPITATES

APPROVED:

R. B. Leane, Jr.  
Major Professor

James L. Carrier  
Minor Professor

James L. Carrier  
Director of the Department of  
Chemistry

Jack Johnson  
Dean of the Graduate School

**THE ADSORPTION OF RADIOACTIVE ISOTOPES  
ON SPECIFIC PRECIPITATES**

**THESIS**

**Presented to the Graduate Council of the  
North Texas State College in Partial  
Fulfillment of the Requirements**

**For the Degree of**

**MASTER OF SCIENCE**

**by**

**Kenneth N. Yarbrough, B. S.**

**Denton, Texas**

**August, 1954**

## TABLE OF CONTENTS

	Page
LIST OF TABLES . . . . .	iv
LIST OF ILLUSTRATIONS . . . . .	v
Chapter	
I. INTRODUCTION . . . . .	1
Factors Affecting Adsorption of Ions on Precipitates Discussion of major factors Discussion of minor factors	
II. EXPERIMENTAL PROCEDURE AND RESULTS . . .	11
General Procedure	
Results	
Investigation with P <sup>32</sup>	
Investigation with I <sup>131</sup>	
Investigation with Ba <sup>140</sup> -La <sup>140</sup>	
Investigation with Ce <sup>144</sup> -Pr <sup>144</sup>	
Investigation with Mixed Isotopes	
III. SUMMARY OF RESULTS . . . . .	50
Characteristics of curves	
Change of charge effect	
Effect of addition of other materials	
Suggestions and Applications	
BIBLIOGRAPHY . . . . .	55

# LIST OF TABLES

Table	Page
1. Carrying of the ThB by $\text{CaSO}_4$ . . . . .	6
2. Adsorption of ThB ( $\text{Pb}^{212}$ ), $\text{MgTh}_2$ ( $\text{Ac}^{228}$ ), and ThX ( $\text{Ra}^{224}$ ) on Silver Halides . . . . .	8
3. Recommended Daily Tolerance Dose . . . . .	17
4. Normalization Factors for $\text{P}^{32}$ with Initial Volume before Addition of Titrant Equal to 60.0 Ml. . . . .	20
5. Radiations of $\text{I}^{131}$ in mev . . . . .	27
6. Normalization Factors for $\text{I}^{131}$ . . . . .	28
7. Radiations from $\text{Ba}^{140}$ - $\text{La}^{140}$ in mev . . . . .	33
8. Normalization Factors for $\text{Ba}^{140}$ - $\text{La}^{140}$ with Initial Volume before Addition of Titrant Equal to 100.0 Ml. . . . .	34
9. Radiations from $\text{Ce}^{144}$ - $\text{Pr}^{144}$ in mev . . . . .	40
10. Normalization Factors for $\text{Ce}^{144}$ - $\text{Pr}^{144}$ with Initial Volume before Addition of Titrant Equal to 100.0 Ml. . . . .	41
11. Normalization Factors for a Mixture of $\text{Ce}^{144}$ - $\text{Pr}^{144}$ and $\text{P}^{32}$ with Initial Volume before Addition of Titrant Equal to 100.0 Ml. . . . .	47
12. Curve Types . . . . .	51

## LIST OF ILLUSTRATIONS

Figure	Page
1. AgCl Crystal, Interlaced Cubic Structure . . .	1
2. Silver Chloride Crystal in Excess Potassium Chloride . . . . .	5
3. Silver Chloride Crystal in Excess Silver Chloride . . . . .	5
4. Apparatus . . . . .	12
5. Water Blank Curve for Radiophosphorous . . . .	19
6. $\text{Ag}_3\text{AsO}_4$ in the Presence of $\text{P}^{32}$ . . . . .	21
7. $\text{AgCNS}$ in the Presence of $\text{P}^{32}$ . . . . .	22
8. $\text{AgCl}$ in the Presence of $\text{P}^{32}$ . . . . .	23
9. $\text{AgIO}_3$ in the Presence of $\text{P}^{32}$ . . . . .	24
10. $\text{Ag}_3\text{PO}_4$ in the Presence of $\text{P}^{32}$ . . . . .	25
11. $\text{BaSO}_4$ in the Presence of $\text{P}^{32}$ . . . . .	26
12. Water Blank Curve for $\text{I}^{131}$ . . . . .	27
13. $\text{AgCl}$ in the Presence of $\text{I}^{131}$ . . . . .	29
14. $\text{AgIO}_3$ in the Presence of $\text{I}^{131}$ . . . . .	30
15. $\text{AgCNS}$ in the Presence of $\text{I}^{131}$ . . . . .	31
16. $\text{BaSO}_4$ in the Presence of $\text{I}^{131}$ . . . . .	32
17. Water Blank Curve for $\text{Ba}^{140}\text{-La}^{140}$ . . . . .	34

# LIST OF ILLUSTRATIONS--Continued

Figure	Page
18. AgCNS in the Presence of Ba <sup>140</sup> -La <sup>140</sup> . . . . .	35
19. AgIO <sub>3</sub> in the Presence of Ba <sup>140</sup> -La <sup>140</sup> . . . . .	36
20. BaSO <sub>4</sub> in the Presence of Ba <sup>140</sup> -La <sup>140</sup> . . . . .	37
21. BaSO <sub>4</sub> in the Presence of Ba <sup>140</sup> -La <sup>140</sup> and Excess La(NO <sub>3</sub> ) <sub>3</sub> as Carrier . . . . .	38
22. BaSO <sub>4</sub> in the Presence of Ba <sup>140</sup> -La <sup>140</sup> and Excess NaNO <sub>3</sub> . . . . .	39
23. Water Blank Curve for Ce <sup>144</sup> -Pr <sup>144</sup> . . . . .	41
24. AgCNS in the Presence of Ce <sup>144</sup> -Pr <sup>144</sup> . . . . .	42
25. AgIO <sub>3</sub> in the Presence of Ce <sup>144</sup> -Pr <sup>144</sup> . . . . .	43
26. BaSO <sub>4</sub> in the Presence of Ce <sup>144</sup> -Pr <sup>144</sup> . . . . .	44
27. Repetition of the Titration Shown in Figure 26 . . . . .	45
28. Water Blank Curve for Mixture of Ce <sup>144</sup> -Pr <sup>144</sup> and P <sup>32</sup> Tracers . . . . .	46
29. AgCNS in the Presence of a Mixture of Ce <sup>144</sup> -Pr <sup>144</sup> and P <sup>32</sup> . . . . .	48
30. BaSO <sub>4</sub> in the Presence of a Mixture of Ba <sup>140</sup> -La <sup>140</sup> and I <sup>131</sup> . . . . .	49

## CHAPTER I

### INTRODUCTION

In the beginning we must define the adsorption process. It is neither strictly a chemical nor a physical phenomenon but possesses the characteristics of both. The qualitative picture presented here will serve as a basis for the quantitative investigation which is the subject of this thesis.

We may see how adsorption occurs if we examine the crystal structure of some ionic compounds. In this case let us use silver chloride which exists as an interlaced simple cubic crystal as shown in Figure 1.

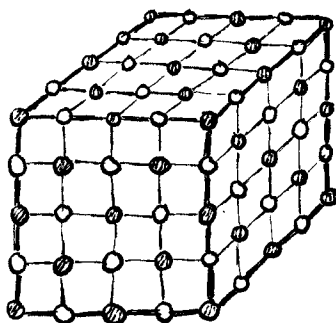


Fig. 1.--AgCl crystal, interlaced cubic structure (  $\odot$  represents silver ion;  $\circ$  represents chloride ion).

We can see that each silver ion is surrounded by six chloride ions, and each chloride ion is surrounded by six silver ions. There exists a balance of coulombic forces

of attraction and repulsion here, so that the crystal lattice is stable within the limits of atomic vibrational motions. Each ion has a symmetric spherical electromotive force field with which it influences surrounding ions. The amount of influence it may have depends upon its size, charge, and distance from surrounding ions. Inside the lattice the force fields of the silver and chloride ions are completely balanced. But, of course, there must be a face to this crystal. What happens with respect to these ionic force fields at this interface? If there are silver and chloride ions in the solution bathing the face they will be attracted to the structure, and crystal growth will occur. The limit to this crystal growth becomes apparent when we consider solubility-product phenomena. There will be a definite concentration of ions in solution which will not be incorporated in the crystal lattice. And the crystal will still have an interface full of unbalanced force fields. Naturally we would expect the ions remaining in the solution to approach the interface during their thermal wanderings. Also we would expect the unbalanced force fields to attract them and hold them loosely at the interface.

Now let us suppose that there are ions other than those of silver and chloride in the solution. Furthermore, let us say that these ions are nearly the same size and have the same charge as the chloride ions. These alien ions will also encounter the interface and its force fields. It is possible



that the alien ions will be attracted and held at the interface due to their similarity to chloride ions. Then the alien ions may be carried by the following processes according to Wahl and Bonner.<sup>1</sup>

- a) Isomorphous Replacement. The tracer is incorporated into the crystal lattice, presumably isomorphously since macro amounts of the tracer and carrier compounds form isomorphous mixed crystals.
- b) Adsorption. The tracer is adsorbed on the surface of a precipitate.
- c) Anomalous-Mixed-Crystal Formation. The tracer is apparently incorporated into the crystal lattice even though macro amounts of the tracer and carrier compounds do not form isomorphous mixed crystals.
- d) "Internal Adsorption." The tracer is apparently adsorbed on surfaces of growing crystals, the result being a discontinuous incorporation of the tracer in the precipitate.

Processes a and b are most clearly understood, and Hahn includes c and d because it is not always possible to assign carrying processes unequivocally to either a or b. The discussion in this section is presented according to Hahn's classification.

In general a tracer ion is efficiently carried by an ionic precipitate if: (1) the tracer ion is isomorphously incorporated into the precipitate, or (2) the tracer ion forms a slightly soluble or slightly dissociated compound with the oppositely charged lattice ion and if the precipitate has a large surface with charge opposite to that of the tracer ion (i.e., presence of excess of the oppositely charged lattice ion).

---

<sup>1</sup>A. C. Wahl and N. A. Bonner, Radioactivity Applied to Chemistry, pp. 104, 105.

### Factors Affecting Adsorption of Ions on Precipitates

In order to investigate the adsorption process we must be familiar with the factors which influence it. The two most important factors are:

- 1) The charge upon the precipitate.
- 2) The solubility of compounds formed from the ion that is coprecipitated and the ions of the precipitate.

Minor factors are:

- 3) Temperature.
- 4) The order of addition of reagents.
- 5) The speed of the precipitation formation.
- 6) In some cases, digestion may affect the adsorption.<sup>2</sup>

### Discussion of Major Factors

The effect of the presence of an excess of one of the lattice ions may be shown by the use of the concept of the electric double layer introduced by Verway, James, Ratner and others.<sup>3</sup> Figure 2 shows how the lattice ions in excess become potential determining as they are attracted to the interface.

---

<sup>2</sup>G. K. Schweitzer and I. B. Whitney, Radioactive Tracer Techniques, p. 125.

<sup>3</sup>Wahl and Bonner, op. cit., p. 124.

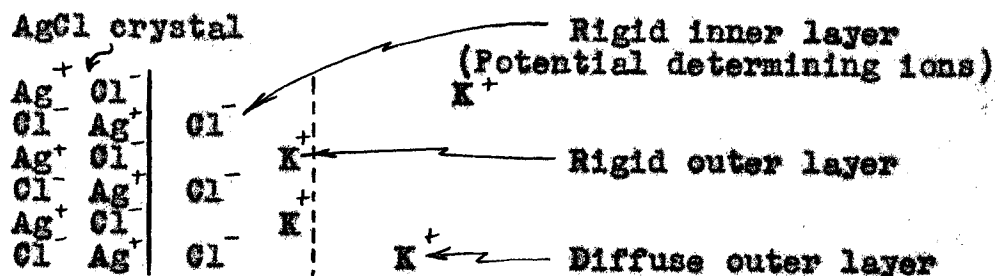


Fig. 2.--Silver chloride crystal in excess potassium chloride.

We can see that the adsorbed chloride ions in the rigid inner layer are held by the coulombic forces between them and the silver ions in the lattice. The rigid outer layer of potassium ions is held more loosely in the same fashion. The charge on the crystal then depends upon the number and charge of potential determining ions. Adsorption of an alien ion into the outer electric layer depends upon the coulombic potential of the adsorbed ions in the rigid inner layer. It also depends upon the structure of the lattice and the distance of closest approach. In Figure 2 the alien ions adsorbed are positive. They might also be negative as in Figure 3.

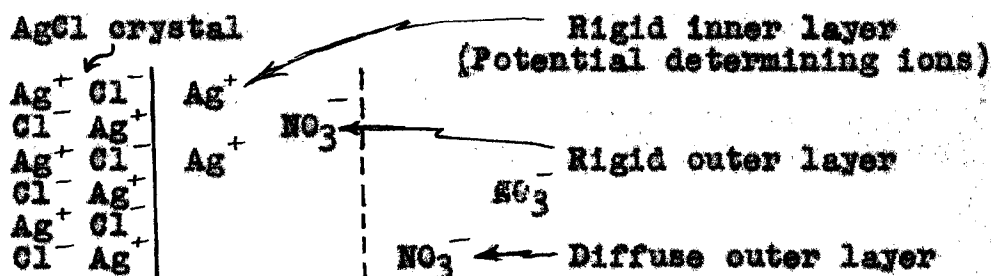


Fig. 3.--Silver chloride crystal in excess silver nitrate.

Any ion which can fit into the crystal lattice is classed as potential determining. It does not follow that this ion must be identical with lattice ions. The specifications are that it must be of a suitable size and charge to allow it to fit into this lattice. The potential determining ion must be identical with lattice ions or capable of undergoing replacement with them.

Table 1<sup>4</sup> illustrates the importance of an excess of the anion  $\text{SO}_4^{=}$  needed to produce the negative charge on the surface of  $\text{CaSO}_4$  necessary for carrying cations.

TABLE 1  
CARRYING OF THE ThB BY  $\text{CaSO}_4$

Excess $\text{Ca}^{++}$	Excess $\text{SO}_4^{=}$	ThB Carried
600% 10%	5% 900%	1.7% 5.2% 88.0% 98.0%

It can be seen that ThB is carried efficiently only when the  $\text{SO}_4^{=}$  ion is in excess.

<sup>4</sup>G. Friedlander and J. W. Kennedy, Introduction to Radiochemistry, p. 265.

The effect of the solubility of compounds formed from the ion that is coprecipitated and the ions of the precipitate has been previously discussed in the defining of different types of adsorption. It is apparent from the consideration of the different types of adsorption that solubility is dependent upon effects due to charge, polarization, and size. Another effect which must be considered is energy of hydration. If these properties of the tracer and oppositely charged lattice ion result in a strong interaction that leads to an insoluble compound or stable complex, this same strong interaction most probably leads to adsorption in the rigid part of the outer electric double layer.<sup>5</sup>

The work of L. Impre<sup>6</sup> shows the effects of solubility upon the adsorption process. He studied the adsorption of ThX(Ra<sup>224</sup>), mesothorium 2(Ac<sup>228</sup>), and ThB(Pb<sup>212</sup>) on the silver halides. The silver halides were shaken with solutions of the radioactive nuclides, separated by filtration through a membrane, and analyzed for their activity. The results are shown in Table 2.

---

<sup>5</sup>Wahl and Bonner, op. cit., p. 128.

<sup>6</sup>L. Impre, Phy. Chem. A153, 127 (1931).

TABLE 2

ADSORPTION OF ThB ( $\text{Pb}^{212}$ ), MesTh<sub>2</sub> ( $\text{Ac}^{228}$ ), AND  
ThX ( $\text{Ra}^{224}$ ) ON SILVER HALIDES\*

Silver Halide	% Thorium B Adsorbed	% Mesothorium 2 Adsorbed	% Thorium X Adsorbed
AgCl	62.2	4.26	0.45
AgBr	93.8	37.7	3.05
AgI	78.0	75.2	7.9

\*0.0003 mole of AgX shaken several minutes at 0°C with 20 ml solution 0.015fX<sup>-</sup>, 0.005fH<sup>+</sup>, 0.03fX<sup>+</sup>.

We can see that mesothorium 2 and thorium X are not as readily adsorbed as thorium B. The halides of mesothorium 2 and thorium X are soluble, but the halides of thorium B are only slightly soluble. Also mesothorium 2, having three positive charges is adsorbed to a greater extent than thorium X, which has two positive charges. The fractions of mesothorium 2 and thorium X adsorbed vary regularly, increasing with decreasing solubility of the silver halide. This may be due in part to the greater polarization effect  $\text{Ac}^{+++}$  and  $\text{Ra}^{++}$  have on the heavier halide ions. The polarizability of the halide ion increases with increasing size of the ion.

#### Discussion of Minor Factors

If the frequency with which ions are brought in contact with the interface force fields is a function of their thermal wandering, temperature dependence in adsorption processes is to be expected. It is important that the temperature effect

be known or that the temperature be held constant. The order of addition of reagents determines whether the potential determining ion is positive or negative on either side of the equivalence point and, therefore, determines whether adsorption occurs before or after the equivalence point. In the case of surface adsorption the alien ions may be displaced if lattice ions of like charge are brought to excess concentration. While the number of alien ions adsorbed and the number displaced might be nearly the same, the time rates of adsorption and displacement could be quite different. Therefore the order of addition of reagents becomes increasingly important as the time allowed for adsorption or displacement is shortened. In the case of isomorphous adsorption the order of addition of reagents is not so important, since displacement is not likely to occur during a short time.

Since the adsorption process occurs on near contact of precipitate interface and charged ion, we must expect some time dependence. The speed of precipitate formation determines the rate of adsorption, since it determines the rate of crystal growth and the size of individual crystals. Adsorption varies directly with the precipitate's area to unit volume ratio.

This ratio is dependent upon the conditions affecting precipitate formation. The effects of changing these conditions must be known, or the conditions must not be allowed to change throughout a quantitative investigation. Stirring rate,

rate of flow of titrant, and temperature are controllable factors affecting precipitate formation.

Over a long period of time adsorption may be affected due to digestion. The time intervals allowed in experimental work presented in this paper are not of sufficient length to allow digestion to occur to an appreciable extent.

The purpose of this investigation is to reveal the effects of the forementioned factors affecting adsorption on some specific precipitates. It is hoped that the choice of precipitate types will enable extension of the information gained here to other precipitates similar to those investigated.



## CHAPTER II

### EXPERIMENTAL PROCEDURE AND RESULTS

In order to make a quantitative determination by volumetric methods the following conditions are necessary:<sup>1</sup>

- 1) The reaction should quickly go to completion.
- 2) There should be only one reaction taking place.
- 3) There should be a marked change in some property of the solution at the stoichiometric point.
- 4) There should be an indicator available which will show the change at the stoichiometric point.

Difficulty with volumetric precipitation reactions is due to the lack of indicators which show the stoichiometric point. All the reactions investigated in this thesis are precipitation reactions. The indicators employed were carrier-free radioactive isotopes in tracer concentrations.

As a precipitate is formed in the presence of a radioactive isotope ions of the tracer isotope may be adsorbed. It is possible with surface adsorption that a marked change in the amount of tracer carried by the precipitate might occur at the stoichiometric point. If the charge on the precipitate is opposite the charge of the radioactive ion

---

<sup>1</sup>W. C. Pierce and E. L. Haenisch, Quantitative Analysis, p. 292.

before the stoichiometric point, adsorption should increase as the amount of precipitate increases. After the stoichiometric point the potential determining ions will have changed causing reversal of the charge on the precipitate. Some of the adsorbed radioactive ions might then be displaced. Such a change is not likely to be noticed with isomorphous adsorption.

Figure 4 schematically shows the apparatus used in this investigation.

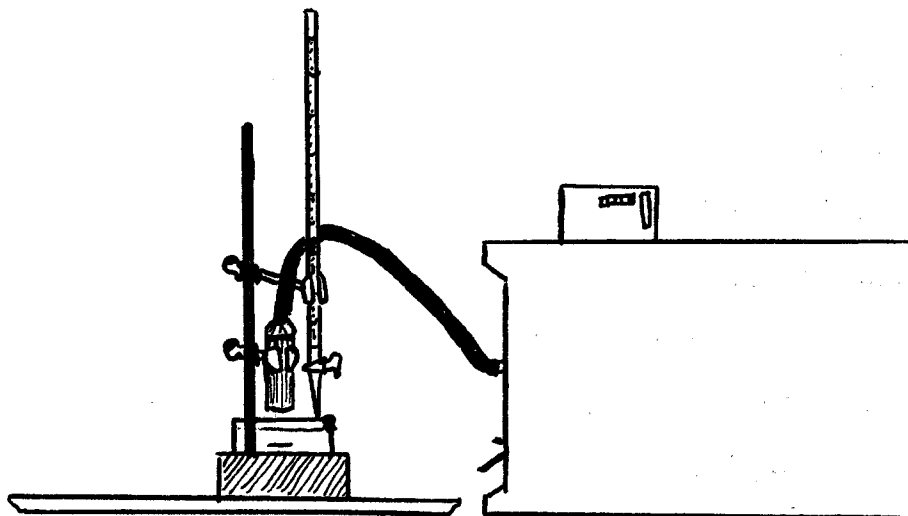


Fig. 4--Apparatus

The reactions were carried out in cylindrical crystallizing dishes which were fifty millimeters deep and one hundred millimeters in diameter. For each reaction the dish was mounted on the top of a magnetic stirring device. In order that each dish should be placed in exactly the same position

as the others, a circle corresponding to the circumference of the dishes was drawn on the stirring unit. The stirring rate was kept constant throughout the entire investigation. Activity in the solution was followed by the counter tube mounted above the dish. The tube was mounted in a fixed position so that the geometry of the situation was held constant. A measured quantity of one of the reactants was added from a burette mounted above the dish. The position of the burette was fixed, and the rate of flow of titrant was kept as constant as possible.

Pulses from the counter tube were received and recorded by a decade scaling unit. An electric timer was started by the same switch that activated the decade unit.

#### General Procedure

A blank was run in order to determine the total effect of the following factors:

- 1) Dilution of the active solution during the titration.
- 2) Change in height of the active solution during addition of the titrant.
- 3) Passing time allowing possible adsorption of the activity on the surface of the dish.

The procedure for running the blank was identical with that for the reactions, except distilled water was used in the burette as titrant and in the dish as solvent for the radioactive isotope.

The procedure for running the reaction determination was as follows:

- 1) Fix the concentration of the reactant in the dish so that the stoichiometric point will theoretically be at 25.0 ml. titrant.
- 2) Take a background count.
- 3) Add radioactive isotope until the activity of the solution reaches the desired level.
- 4) Bring the total volume of the solution to a fixed value.
- 5) With the apparatus in place as shown in Figure 4 record the activity of the solution in the dish.
- 6) Begin the titration. Titrant is to be added in 5.0 ml. portions until 20.0 ml. have been added. It is then added in 2.5 ml. portions until 30.0 ml. have been added, after which two 5.0 ml. and one 10.0 ml. portions are added.
- 7) The solution is stirred at a constant rate for 2.0 minutes after each addition of titrant. A time interval of 2.0 minutes is then allowed for settling of the precipitate. The activity of the solution is then measured over a 1.00 minute time interval.
- 8) After the titration is completed the dish is removed and a background count is taken.

The concentrations of reactants were made low enough to insure that the precipitates formed would occupy a small volume with respect to the total volume of solution in the dish. After settling of the precipitate the solution above it acted as an absorber for beta and alpha particles. Therefore the only activities observed could have been alpha and/or beta particles from the top few millimeters of the solution and/or gamma emission from the total contents of the dish.

Since each titration took little more than one hour, constant temperature was easily maintained. Room temperature was checked and found to be constant over the determination time.

Possible effects due to reversal of the order of addition of reagents were investigated. Each precipitate was formed twice, once for each reagent as titrant.

The radioactive isotopes used as indicators were introduced only in tracer concentrations. Macro amounts of the tracers might form precipitates with some of the reagents used. However, concentrations of the isotopes were so low that the solubility-product constants of possible precipitates were not exceeded.

Adequate precautions in handling radioactive isotopes were taken to insure the safety of the investigator. The following rules for laboratory procedure were followed when they applied to the situation:

- 1) . . . wear protective clothing in the laboratory--  
. . . keep it there.
- 2) Wear pocket chambers during all laboratory periods.  
. . . Avoid jarring them severely.
- 3) Do not use the mouth for pipetting and do not put it in contact with any other apparatus in the laboratory.
- 4) Do not smoke or eat in the laboratory.
- 5) Use hood in all cases where radioactive material may be lost by volatilization, by dusting, or by spraying or spattering. Work with closed containers wherever possible.

- 6) Meter all radioactive samples and determine the safe working distance or shielding procedure before beginning work with them.
- 7) Avoid handling samples in such a way that any radioactive material can be transferred to the hands or other parts of the body.
- 8) Plan your work carefully to minimize any danger of spilling radioactive material. Work over absorbent paper so that if slight losses occur they will be caught by the paper, which is disposable. . . .
- 9) . . .
- 10) If radioactive material should be spilled on the floor, commence taking requisite steps for cleaning it up immediately. . . .
- 11) Meter your working space at the beginning of the working period and again at the end.
- 12) Wear rubber gloves in the laboratory while manipulating active materials.
- 13) All radioactive waste must be disposed of in containers provided especially for this purpose. Accumulated waste is to be buried.<sup>2</sup>

Table 3<sup>3</sup> shows the recommended daily tolerance dose as established by the United States Atomic Energy Commission. Present tolerance levels are lower than those shown below. The tolerance level for beta and gamma radiations is now 0.3 rep per week. Tolerance doses in the table below are expressed in roentgens (r), roentgen equivalents mammal (rem), and roentgen equivalents physical (rep).

---

<sup>2</sup>E. Bleuler and G. J. Goldsmith, Experimental Nucleonics, pp. 14-15.

<sup>3</sup>Ibid., p. 7.

TABLE 3  
RECOMMENDED DAILY TOLERANCE DOSE

Type of Radiation	Tolerance Dose for 8-hr Day			
	r	rem	rep	n
X rays	0.1	0.1	0.1	...
Gamma rays	0.1	0.1	0.1	...
Beta particles	...	0.1	0.1	...
Fast neutrons	...	0.1	0.02	0.01
Slow neutrons	...	0.1	0.02-0.05	...
Alpha particles	...	0.1	0.01	...

This [the roentgen] is a unit of energy dissipation, not a unit of radiation intensity. It is defined as that quantity of X radiation (or gamma radiation) for which the secondary particles emitted per 0.001293 g of air ( $= 1 \text{ cm}^3$  at normal conditions) produce, in air, ions carrying one esu of electricity of either sign. . . .

. . . The derived unit, the roentgen equivalent physical (rep), then, is defined as being that quantity of radiation which suffers an absorption in tissue of 93 erg/g.

Since various types of radiation do not produce precisely the same biological effect, it has been proposed that a second derived unit which takes this factor into account be used. The relative biological effectiveness (RBE) of tissue ionization due to a certain type of radiation is taken as the ratio of the ionization produced by gamma rays to that due to the radiation under consideration which will produce the same biological effects. Unfortunately, up to the present, there are no very good values for RBE in man. Generally a value of unity for beta radiation and values from 5 to 10 for neutrons and alpha particles have been recommended. . . . The derived unit taking these effects into account is the roentgen equivalent mammal (or man) (rem). It is that quantity of radiation which, when absorbed by tissue,

produces an effect equivalent to the adsorption of one roentgen of X radiation or gamma radiation. One rem, then, is equal to 1 rep/RBE; or the energy absorbed with a dose of 1 rem is equal to 93 erg/RBE.<sup>4</sup>

### Results

Four radioactive isotopes were used in this investigation. They were radiophosphorous ( $P^{32}$ ), radioiodine ( $I^{131}$ ), radiobarium-lanthanum ( $Ba^{140}$ - $La^{140}$ ), and radiocerium-praseodymium ( $Ce^{144}$ - $Pr^{144}$ ).

#### Investigation with $P^{32}$

The radiophosphorous used was obtained from the Oak Ridge National Laboratory. It was produced by  $S^{32}$  (n,p)  $P^{32}$  reaction. Its chemical form was phosphate in weak HCl (<0.5N), and it was 99% pure with a high specific activity (~0.025 mg P/mc). The total solids present were less than 5 mg/mc. For our purposes the radiophosphorous was carrier-free. This particular form of  $P^{32}$  is readily available, as it is a stock item. Its price is reasonable at \$1.10 per mc plus \$10.00 service charge per order. The half-life of  $P^{32}$  is 14.30 days, and it is a pure beta emitter giving off beta particles of 1.712 mev.

The water blank curve for radiophosphorous is shown in Figure 5. The following titration curves for  $P^{32}$  as indicator have been normalized at 20.0 ml. titrant with respect to the water blank curve in Figure 5.

---

<sup>4</sup>Ibid., p. 5.



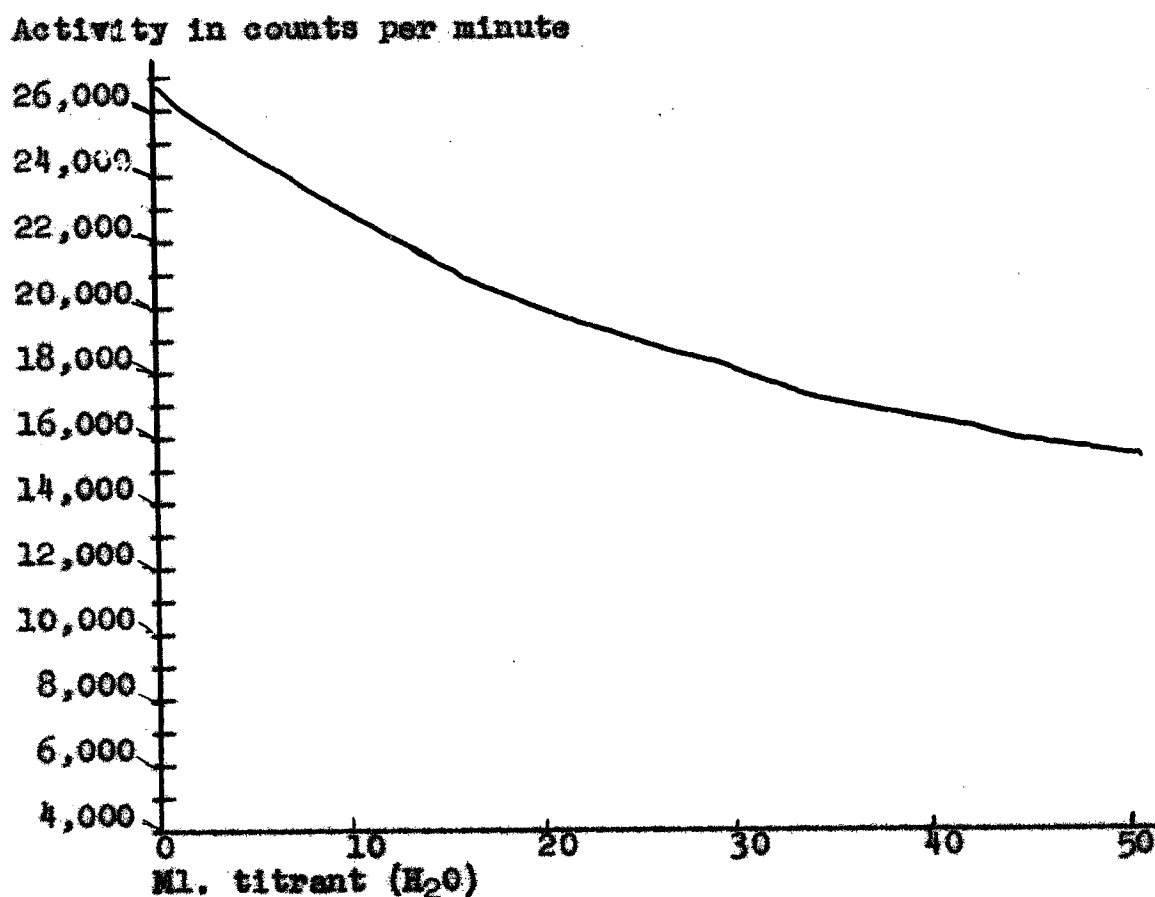


Fig. 5--Water blank curve for radiophosphorous

The effect of normalization was to give a titration curve showing no effects due to dilution upon addition of titrant, change in height due to addition of titrant, and possible adsorption on the surface of the dish over the titration period. The formula for normalization is:

$$\left[ \frac{A}{a_v} \right] M_v = N_v$$

where A is the activity on the water blank curve at 20.0 ml. titrant,  $a_v$  is the activity on the water blank curve at v ml. titrant, and  $N_v$  is the activity on the titration curve at v

ml. titrant.  $N_v$  is the value for the activity on the normalized titration curve.  $\left[ \frac{A}{s_v} \right]$  is called the normalization factor. Table 4 gives the normalization factors obtained from the P32 water blank curve.

TABLE 4

NORMALIZATION FACTORS FOR P32 WITH INITIAL VOLUME BEFORE ADDITION OF TITRANT EQUAL TO 60.0 ML.

ML. Titrant	Normalization Factor
0 . . . . .	0.7850
5 . . . . .	0.8258
10 . . . . .	0.8764
15 . . . . .	0.9505
20 . . . . .	1.0000
22.5 . . . . .	1.0360
25 . . . . .	1.0522
27.5 . . . . .	1.0775
30 . . . . .	1.0955
35 . . . . .	1.1514
40 . . . . .	1.1898
50 . . . . .	1.2753

Division of the activity at volume  $v$  of titrant on the following titration curves by the corresponding normalization factor at that volume yields the unnormalized value of activity experimentally observed.

Due to the random nature of nuclear transitions a statistical error will always be present in measuring activities. The error will be nearly equal to the square root of the measured activity. The statistical errors involved in measuring activity from P32 are small with respect to the activity. They are therefore closely represented by the thickness of the lines drawn to represent the titration curves.

In each titration the radiophosphorous was present in a tracer concentration in the dish. The solution being titrated was always brought to 60.0 ml. total volume with distilled water before beginning the titration.

Figure 6 shows the titration curves obtained by precipitating  $\text{Ag}_3\text{AsO}_4$  in the presence of  $\text{p}^{32}$  as  $\text{PO}_4^{3-}$ .

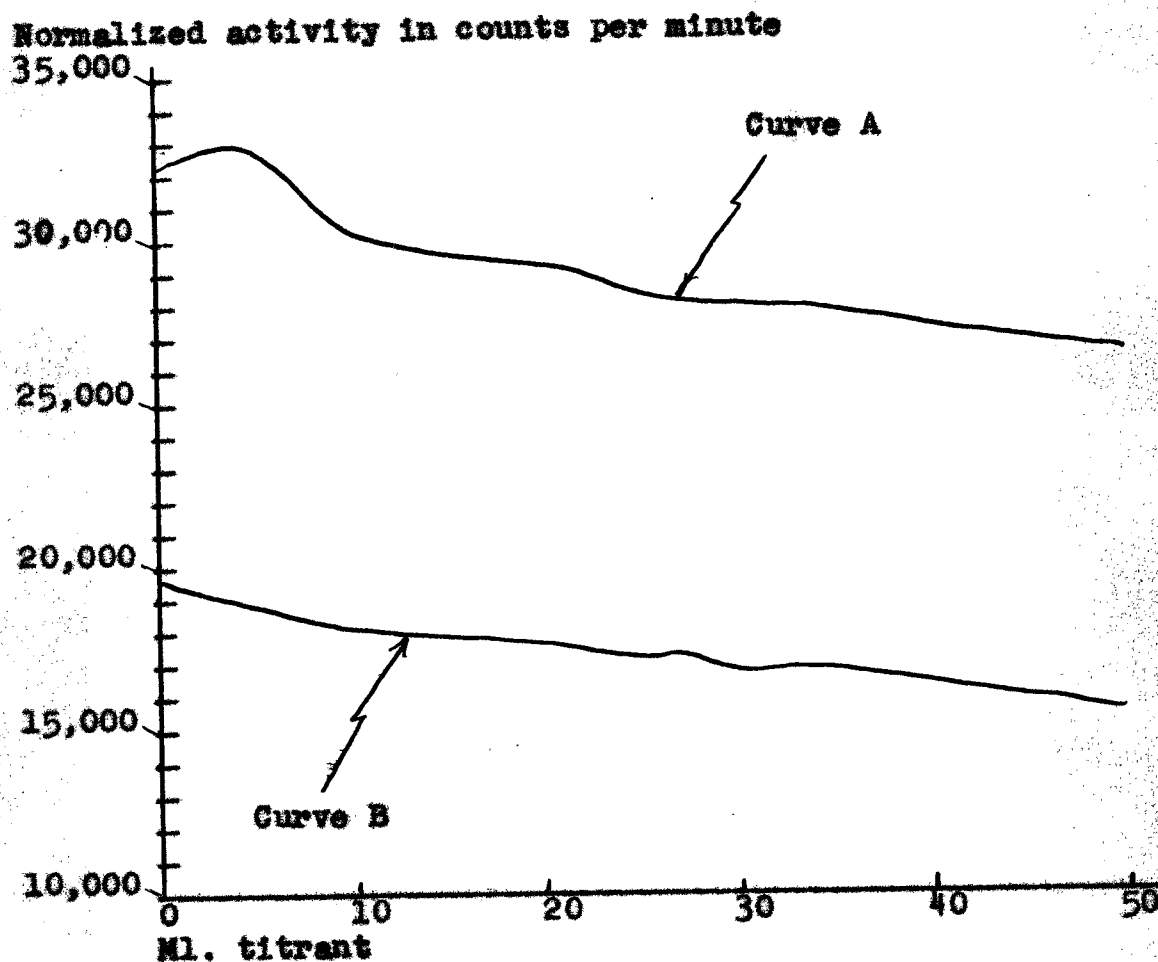


Fig. 6-- $\text{Ag}_3\text{AsO}_4$  in the presence of  $\text{p}^{32}$

The stoichiometric point in curve A is theoretically 16.66 ml. titrant. This is the only exception. The stoichiometric points for all other titration curves in this thesis are

at 25.0 ml. titrant.  $\text{Ag}_3\text{AsO}_4$  is a fine precipitate and complete settling was not obtained.

Curve A in Figure 6 results from adding 0.225 M  $\text{KH}_2\text{AsO}_4$  to a solution containing 12.50 ml. of 0.300 M  $\text{AgNO}_3$ . Curve B in the same figure results from adding 0.150 M  $\text{AgNO}_3$  to a solution containing 25.0 ml. of 0.150 M  $\text{Na}_2\text{HAsO}_4$ .

Figure 7 shows the titration curves obtained by precipitating  $\text{AgCNS}$  in the presence of  $\text{P}^{32}$  as  $\text{PO}_4^{3-}$ .

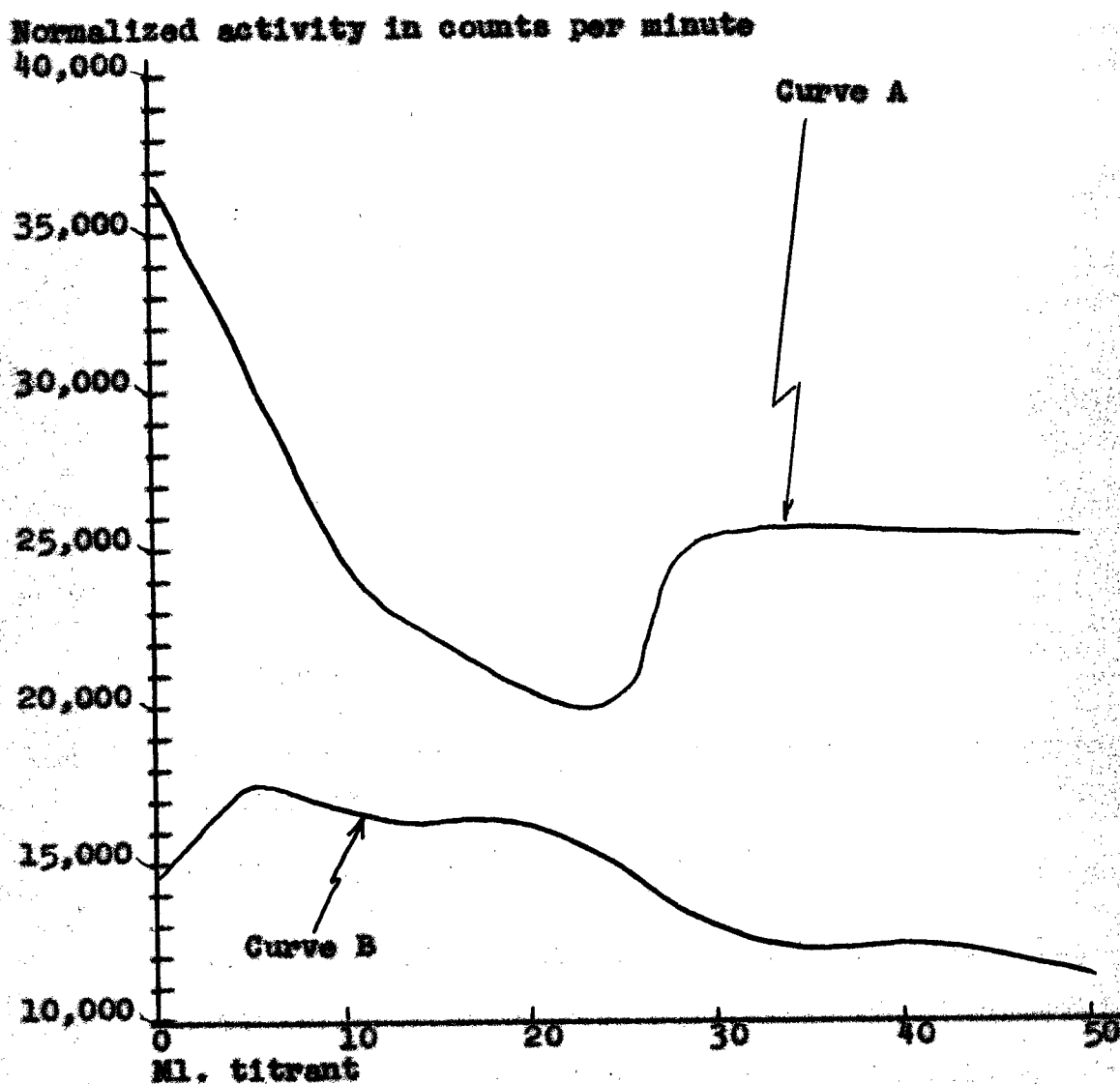


Fig. 7-- $\text{AgCNS}$  in the presence of  $\text{P}^{32}$

Curve A in Figure 7 results from adding 0.150 M NaCNS to a solution containing 12.50 ml. of 0.300 M  $\text{AgNO}_3$ ; curve B results from adding 0.150 M  $\text{AgNO}_3$  to a solution containing 25.0 ml. of 0.150 M NaCNS. The settling was not complete. Most of the precipitate went to the bottom, but enough remained suspended in the solution to make it turbid.

Figure 8 shows the titration curves obtained by precipitating  $\text{AgCl}$  in the presence of  $\text{P}^{32}$  as  $\text{PO}_4^{3-}$ .

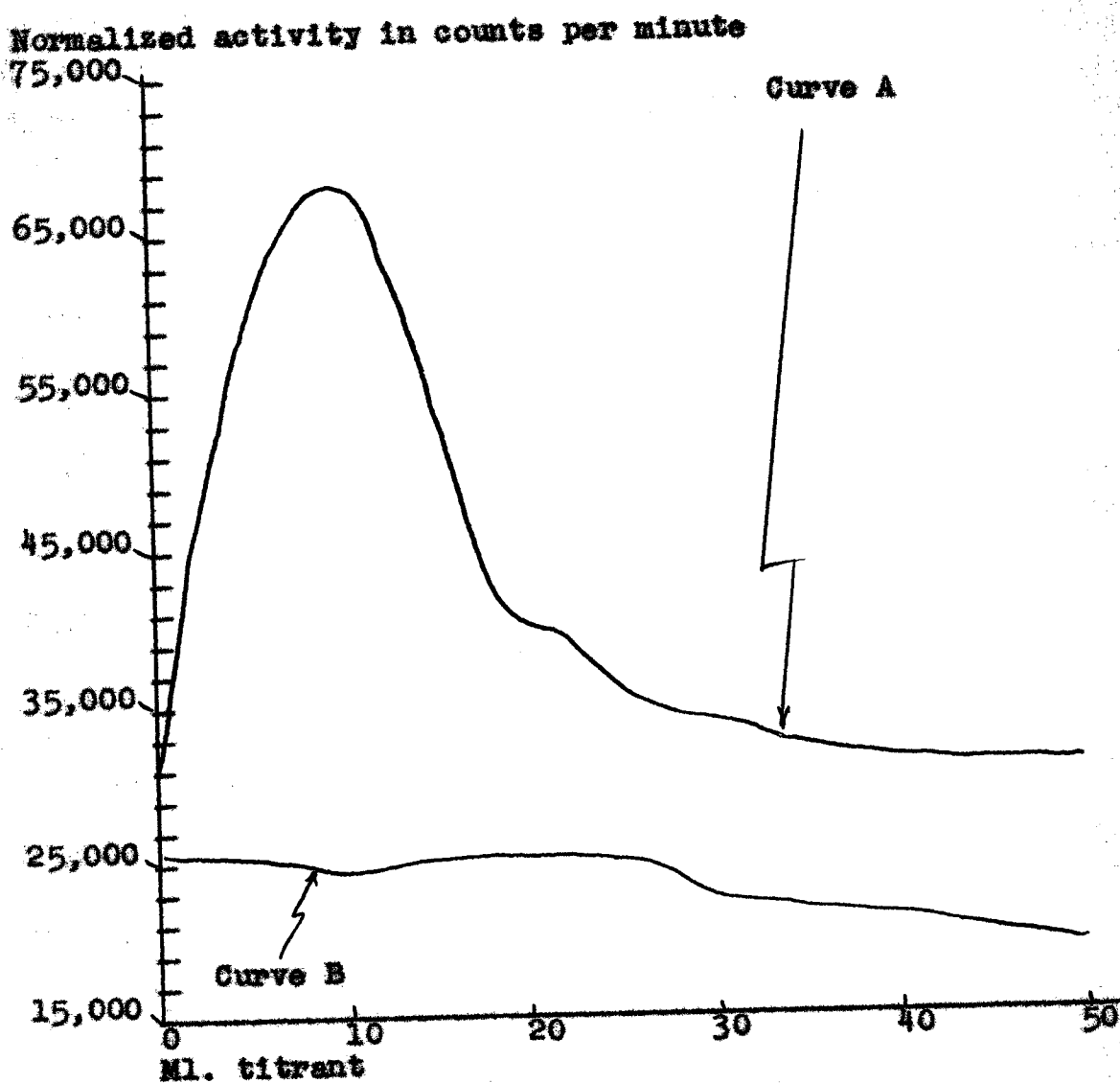


Fig. 8-- $\text{AgCl}$  in the presence of  $\text{P}^{32}$

Curve A results from adding 0.150 M KCl to a solution containing 12.50 ml. of 0.300 M  $\text{AgNO}_3$ . Curve B results from adding 0.150 M  $\text{AgNO}_3$  to a solution containing 25.0 ml. of 0.150 M KCl.

Curds of  $\text{AgCl}$  floated during the titration for curve A. This was prevented in the titration for curve B by the addition of "Joy" liquid detergent. In both titrations some  $\text{Ag}^+$  was reduced to  $\text{Ag}^0$  by photochemical action.

Figure 9 shows the titration curves obtained by precipitating  $\text{AgIO}_3$  in the presence of  $\text{P}^{32}$  as  $\text{PO}_4^{3-}$ .

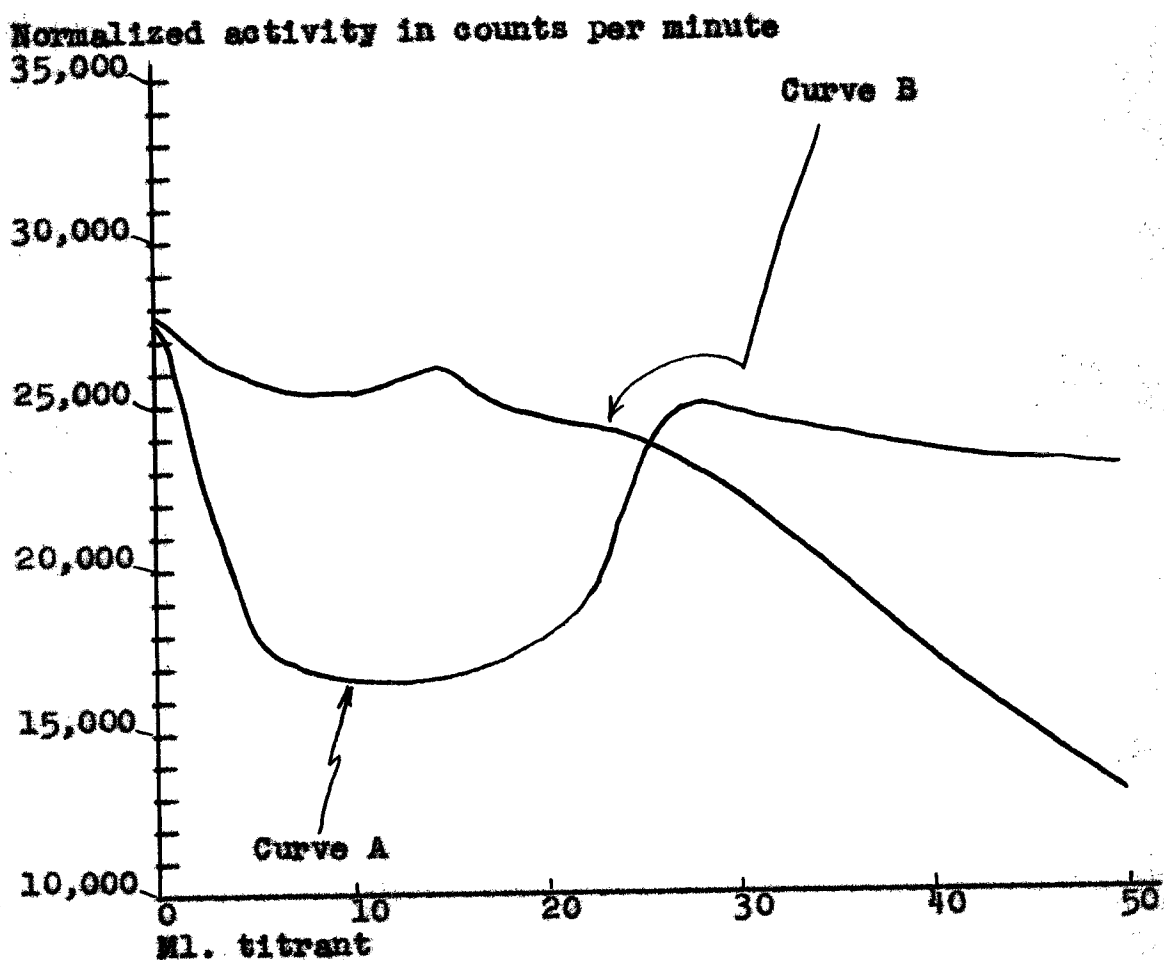


Fig. 9-- $\text{AgIO}_3$  in the presence of  $\text{P}^{32}$

Curve A in Figure 9 results from adding 0.150 M  $\text{NaIO}_3$  to a solution containing 12.50 ml. of 0.300 M  $\text{AgNO}_3$ . Curve B in the same figure results from adding 0.150 M  $\text{AgNO}_3$  to a solution containing 25.0 ml. of 0.150 M  $\text{NaIO}_3$ . Settling of  $\text{AgIO}_3$  was good with very little precipitate left suspended in solution.

Figure 10 shows the titration curves obtained by precipitating  $\text{Ag}_3\text{PO}_4$  in the presence of  $\text{P}^{32}$  as  $\text{PO}_4^{3-}$ .

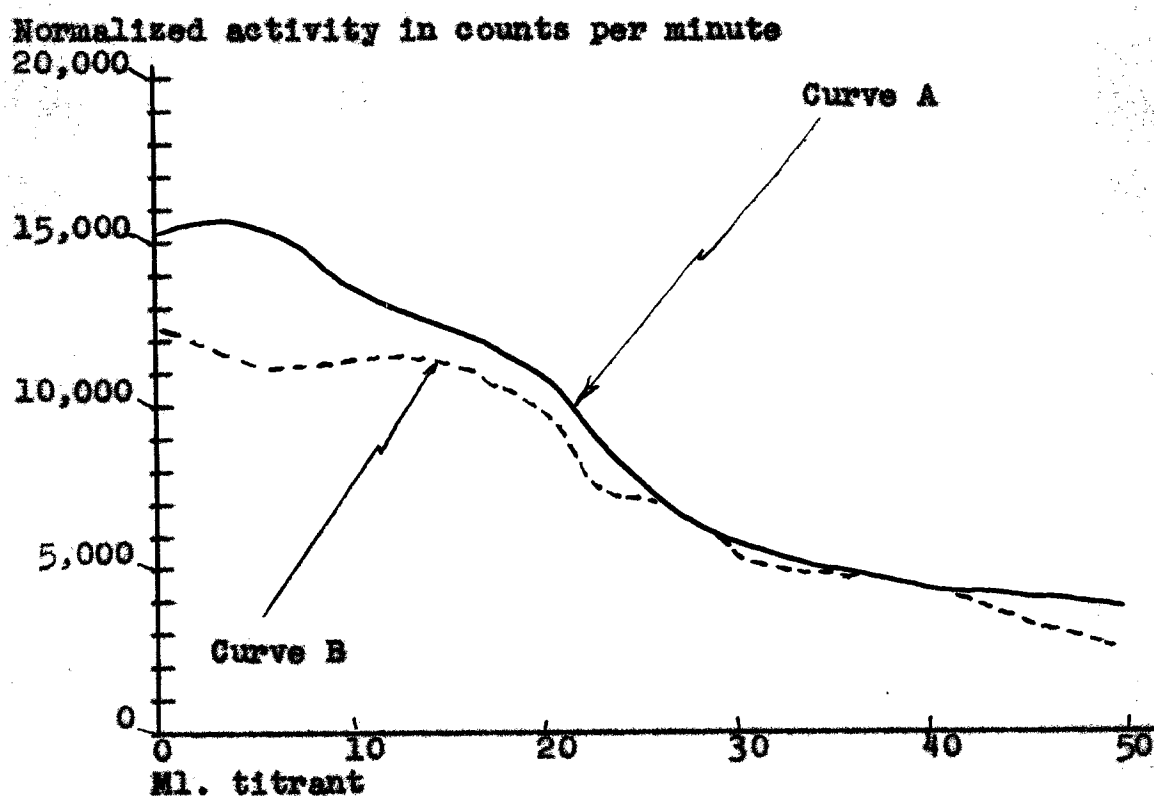


Fig. 10-- $\text{Ag}_3\text{PO}_4$  in the presence of  $\text{P}^{32}$

Curve A results from adding 0.150 M  $\text{AgNO}_3$  to a solution containing 25.0 ml. of 0.150 M  $\text{KH}_2\text{PO}_4$ . Curve B results from adding 0.150 M  $\text{KH}_2\text{PO}_4$  to a solution containing 25.0 ml. of 0.300 M  $\text{AgNO}_3$ .

Settling of the precipitate was very good with very little left in suspension.

Figure 11 shows the titration curves obtained by precipitating  $\text{BaSO}_4$  in the presence of  $\text{P}^{32}$  as  $\text{PO}_4^{3-}$ .

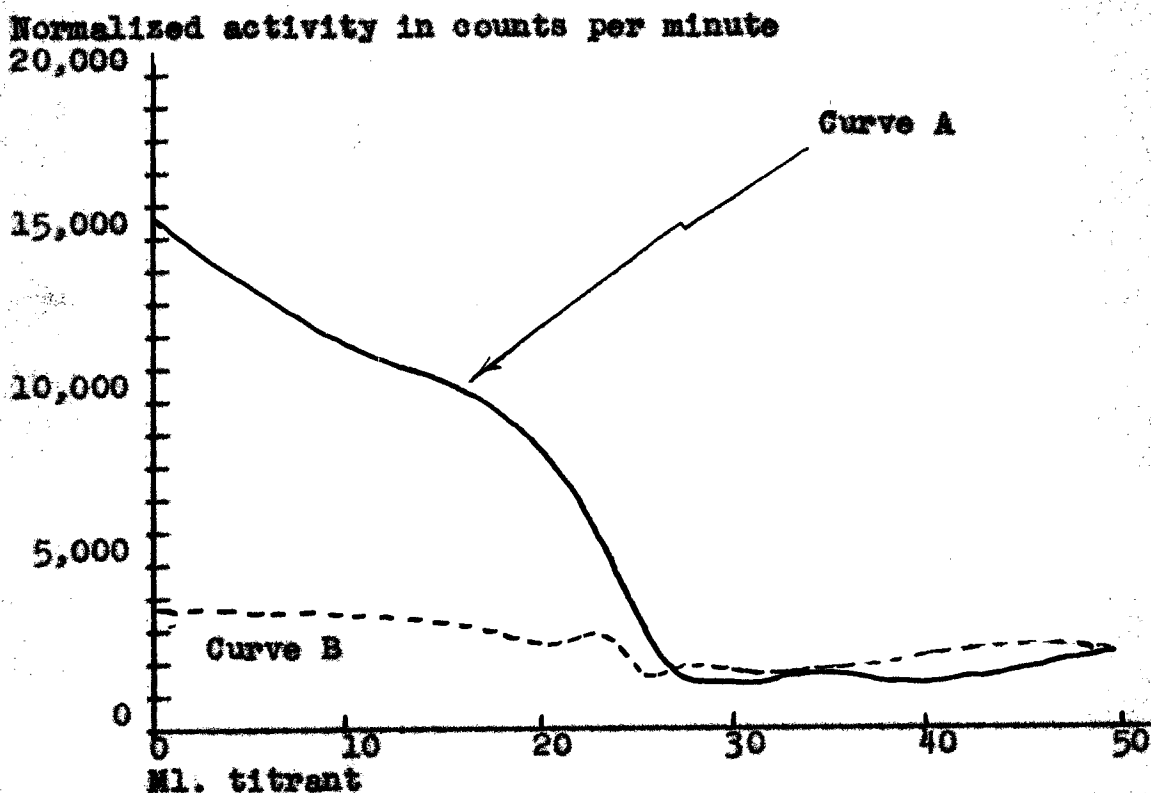


Fig. 11-- $\text{BaSO}_4$  in the presence of  $\text{P}^{32}$

Curve A results from adding 0.100 M  $\text{Ba}(\text{NO}_3)_2$  to a solution containing 25.0 ml. of 0.100 M  $\text{Na}_2\text{SO}_4$ . Curve B results from adding 0.100 M  $\text{Na}_2\text{SO}_4$  to a solution containing 25.0 ml. of 0.100 M  $\text{Ba}(\text{NO}_3)_2$ .

Settling of the precipitate was good with little suspension in solution.



Investigation with  $I^{131}$ 

The radioiodine used was obtained from the Oak Ridge National Laboratory. It was produced by fission and had a half-life of eight days. It was carrier-free in the form of 99% pure NaI in  $Na_2SO_3$  solution of basicity 0.005 N to 0.05 N NaOH. The radiations from  $I^{131}$  are listed in Table 5.

TABLE 5  
RADIATIONS OF  $I^{131}$  IN MEV

Beta	Gamma
0.33 (8%)	0.720
0.60 (89%)	0.364
0.15 (2%)	0.284
0.81 (0.8%)	0.080
	~ 0.16

This particular form of radioiodine is a readily available stock item priced reasonably at \$0.75/mc plus \$10.00 service charge per order.

Figure 12 shows the water blank curve for  $I^{131}$ .

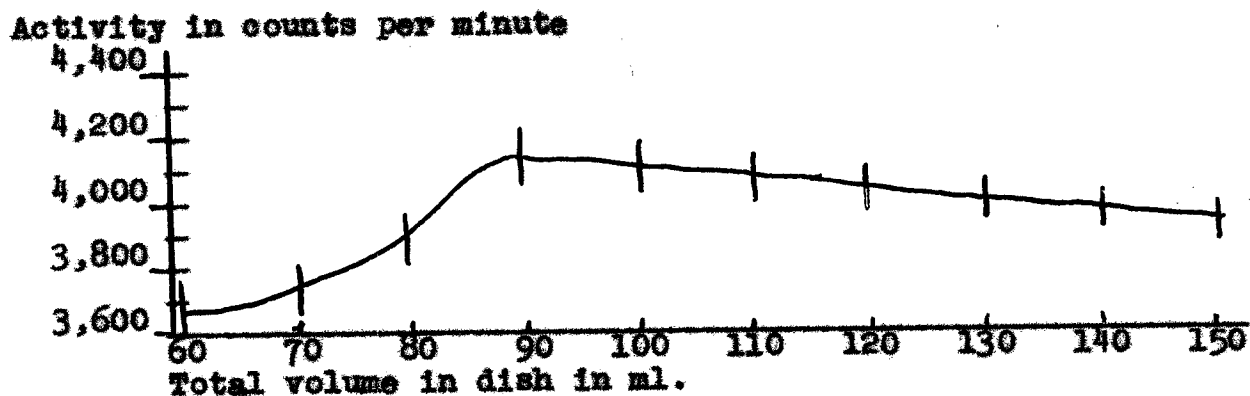


Fig. 12--Water blank curve for  $I^{131}$

Values for normalization factors in Table 6 were derived from the curve in Figure 12.

TABLE 6  
NORMALIZATION FACTORS FOR  $I^{131}$

Ml. Titrant	Normalization Factors for Initial Volume of 60 ml.	Normalization Factors for Initial Volume of 100 ml.
0	1.0525	0.9838
5	1.0434	0.9881
10	1.0336	0.9924
15	1.0212	0.9961
20	1.0000	1.0000
22.5	0.9846	1.0022
25	0.9506	1.0035
27.5	0.9333	1.0062
30	0.9288	1.0084
35	0.9277	1.0135
40	0.9320	1.0160
50	0.9402	1.0250

The statistical errors involved in measuring the activities from  $I^{131}$  are represented by vertical lines through the points on the curves for  $I^{131}$  determinations.

The following titration curves for  $I^{131}$  as indicator have been normalized at 20.0 ml. titrant with respect to the water blank curve in Figure 12.

In the titrations represented in Figures 13 and 14 the solutions being titrated were brought to 60.0 ml. total volume with distilled water before beginning the titration. In the titrations represented in Figures 15 and 16 the solutions being titrated were brought to 100.0 ml. total volume with distilled

water before beginning the titration. The radiiodine was present in a tracer concentration in the dish in each titration.

Figure 13 shows the titration curves obtained by precipitating AgCl in the presence of  $I^{131}$  as  $I^-$ .

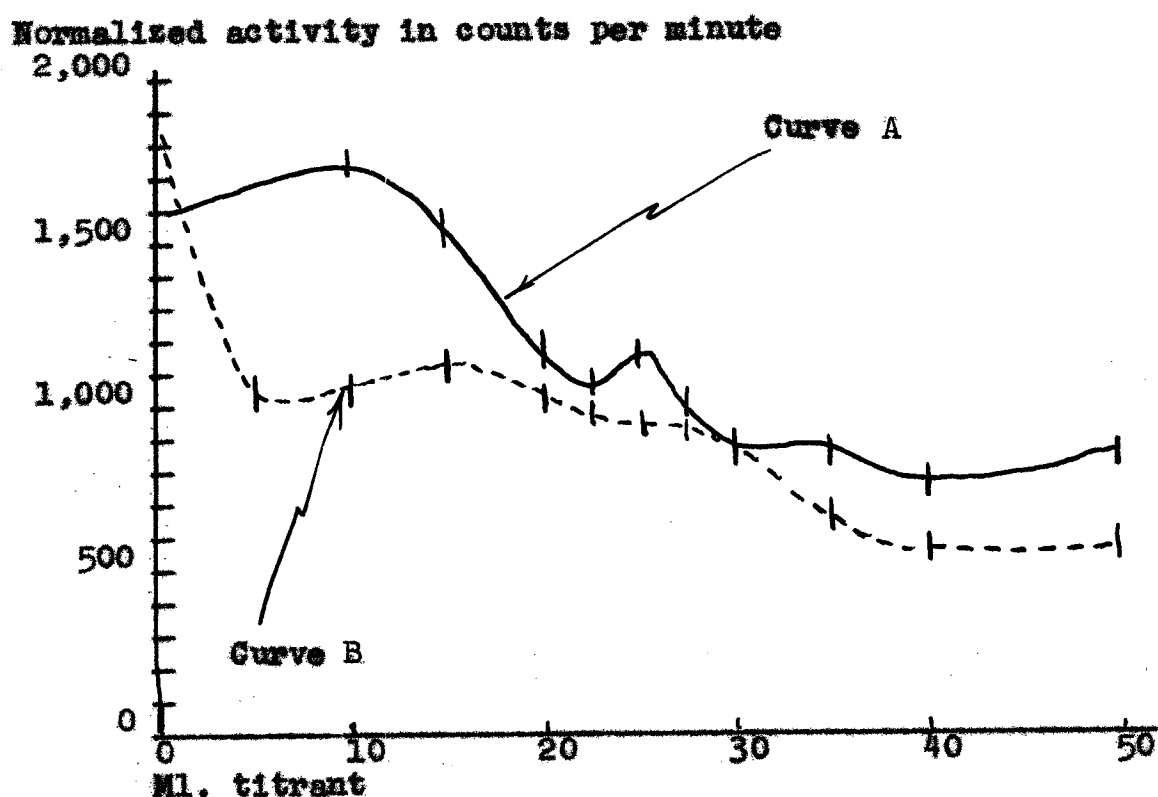


Fig. 13--AgCl in the presence of  $I^{131}$

Curve A results from adding 0.150 M KCl to a solution containing 12.50 ml. of 0.300 M  $AgNO_3$ . Curve B results from adding 0.150 M  $AgNO_3$  to a solution containing 25.0 ml. of 0.150 M KCl.

"Joy" liquid detergent was added to prevent floating curds. However, in the titration for curve A there were a few curds

floating up to 10 ml. titrant. No curds floated in the titration for curve B. Here again Ag was reduced to  $\text{Ag}^0$  by photochemical action.

Figure 14 shows the titration curves obtained by precipitating  $\text{AgIO}_3$  in the presence of  $\text{I}^{131}$  as  $\text{I}^-$ .

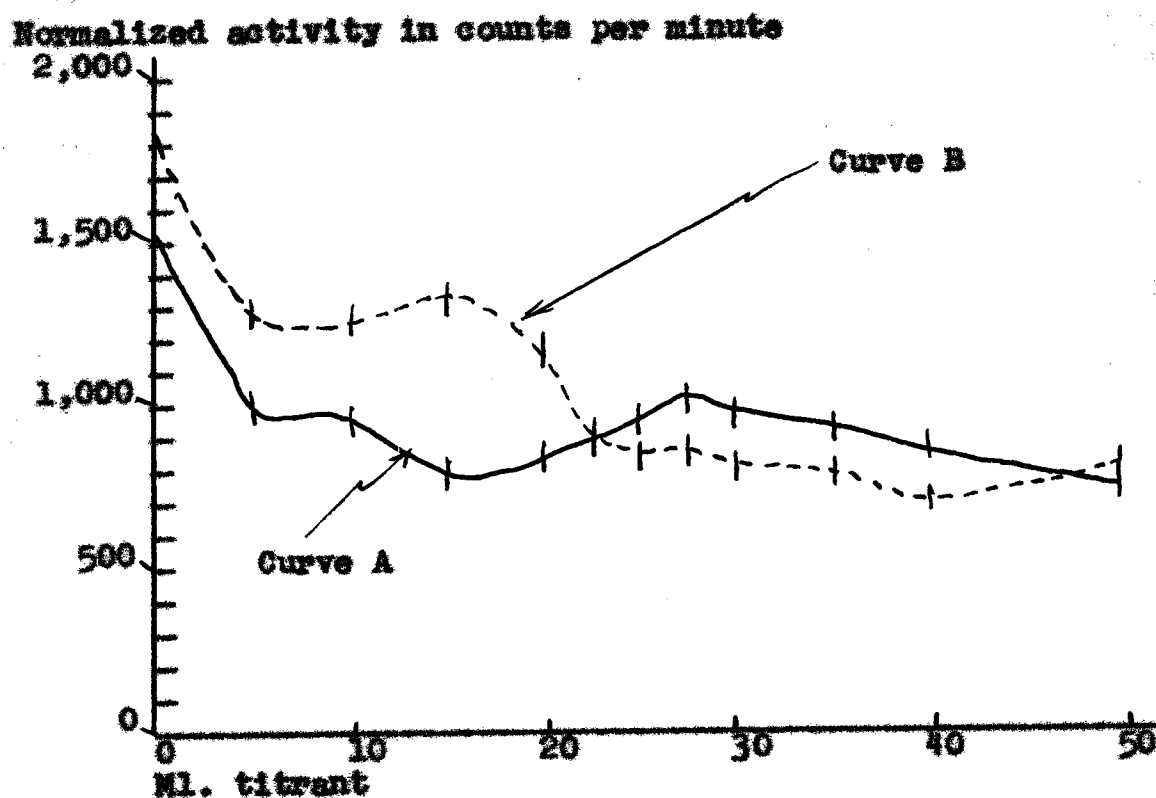


Fig. 14-- $\text{AgIO}_3$  in the presence of  $\text{I}^{131}$

Curve A results from adding 0.150 M  $\text{AgNO}_3$  to a solution containing 25.0 ml. of 0.150 M  $\text{NaIO}_3$ . Curve B results from adding 0.150 M  $\text{NaIO}_3$  to a solution containing 12.50 ml. of 0.300 M  $\text{AgNO}_3$ .

Settling of the  $\text{AgIO}_3$  precipitate was excellent with no noticeable suspension in solution.

Figure 15 shows the titration curves obtained by precipitating AgCNS in the presence of  $I^{131}$  as  $I^-$ .

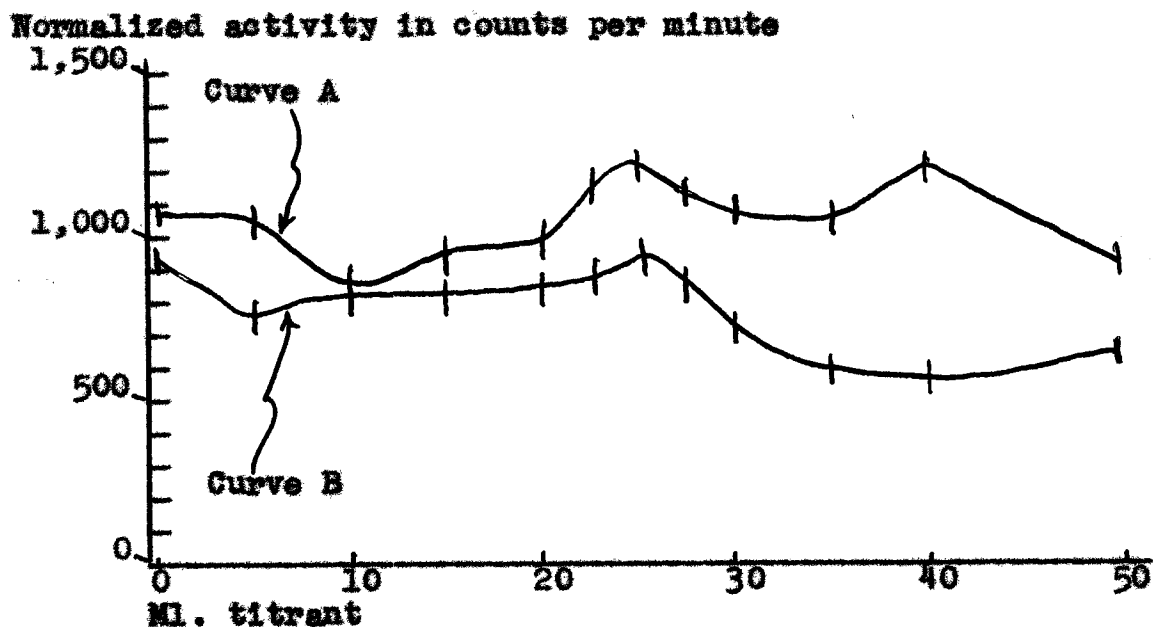


Fig. 15--AgCNS in the presence of  $I^{131}$

Curve A results from adding 0.150 M  $AgNO_3$  to a solution containing 12.50 ml. of 0.300 M NaCNS. Curve B results from adding 0.150 M NaCNS to a solution containing 12.50 ml. of 0.300 M  $AgNO_3$ .

In both titrations the precipitate remained dispersed in solution with poor settling up to 20.0 ml. titrant. Then curds formed and settling became better. However, a few curds remained floating for the remainder of the titrations.

Figure 16 shows the titration curves obtained by precipitating  $BaSO_4$  in the presence of  $I^{131}$  as  $I^-$ .

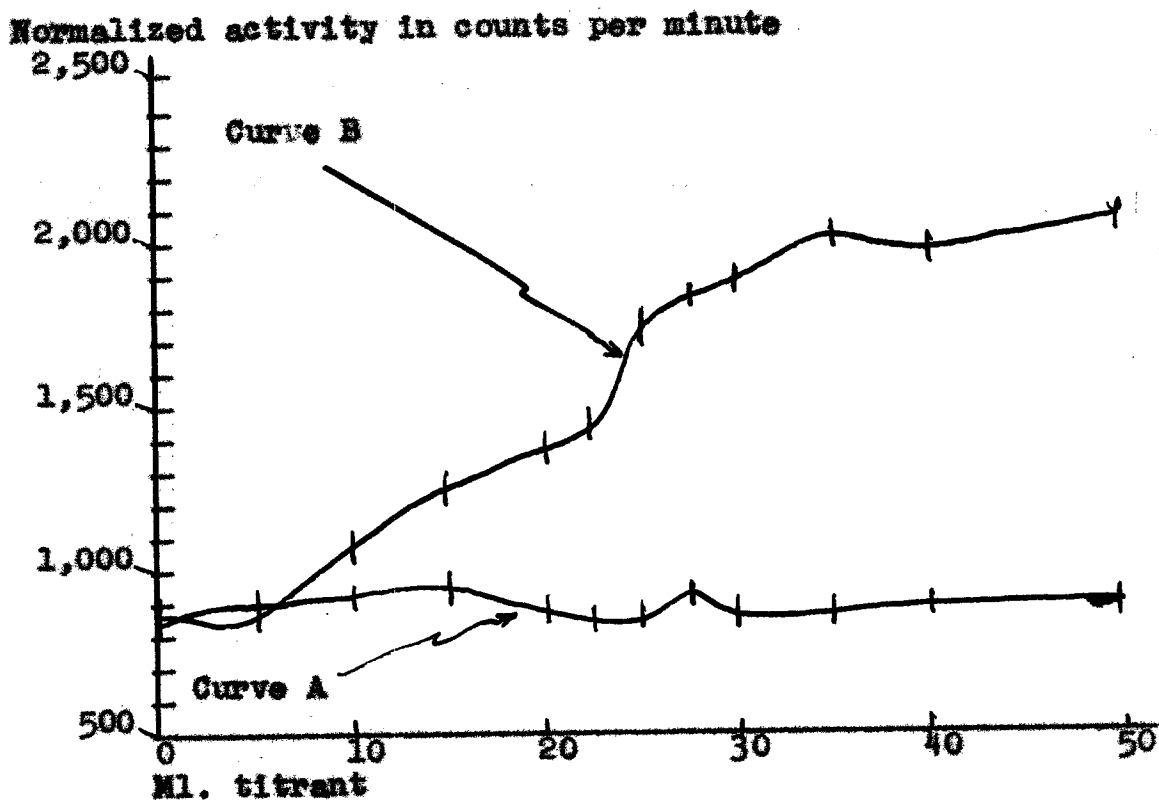


Fig. 16--BaSO<sub>4</sub> in the presence of I<sup>131</sup>

Curve A results from adding 0.100 M Na<sub>2</sub>SO<sub>4</sub> to a solution containing 25.0 ml. of 0.100 M Ba(NO<sub>3</sub>)<sub>2</sub>. Curve B results from adding 0.100 M Ba(NO<sub>3</sub>)<sub>2</sub> to a solution containing 25.0 ml. of 0.100 M Na<sub>2</sub>SO<sub>4</sub>.

Settling was good in the titration for curve A and excellent in the titration for curve B.

#### Investigation with Ba<sup>140</sup>-La<sup>140</sup>

The Ba<sup>140</sup>-La<sup>140</sup> used in this investigation was obtained from the Oak Ridge National Laboratory. It was produced by fission Ba<sup>140</sup> (12.8d)  $\beta \rightarrow$  La<sup>140</sup> to a purity of 98% exclusive of daughter. The chemical form was as chlorides in less

than one normal HCl with no added carrier. Radiations from  $\text{Ba}^{140}\text{-La}^{140}$  are given in Table 7.

TABLE 7  
RADIATIONS FROM  $\text{Ba}^{140}\text{-La}^{140}$  IN MEV

Isotope	Radiations	
	Beta	Gamma
$\text{Ba}^{140}$	0.48 (40%) 1.022 (60%)	0.306 0.160 0.540
$\text{La}^{140}$	1.32 (70%) 1.67 (20%) 2.26 (10%)	0.093 0.335 0.49 0.82 1.6 2.55 (4%) 2.9 (6.1%)

This form of  $\text{Ba}^{140}\text{-La}^{140}$  is processed at three month intervals and priced at \$1.00/mc plus \$10.00 service charge per order. The half-life of  $\text{Ba}^{140}$  is 12.8 days, and the half-life of  $\text{La}^{140}$  is 40 hours.

The water blank curve for  $\text{Ba}^{140}\text{-La}^{140}$  is shown in Figure 17.

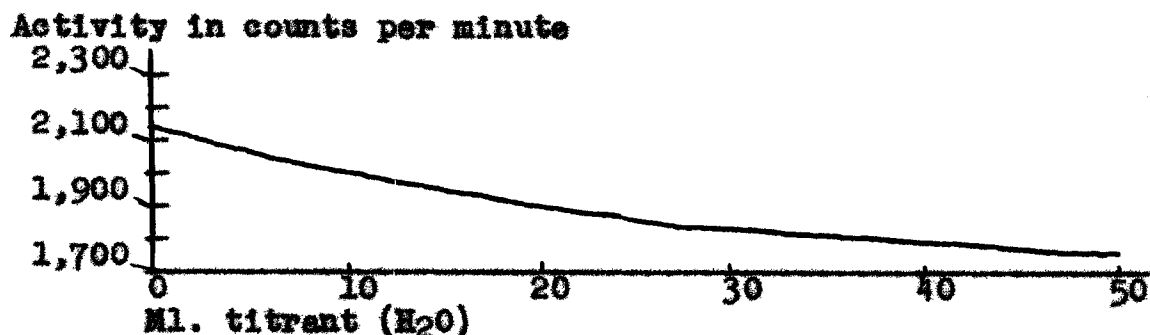


Fig. 17--Water blank curve for  $\text{Ba}^{140}\text{-La}^{140}$

Normalization factors derived from this curve are shown in Table 8.

TABLE 8

NORMALIZATION FACTORS FOR  $\text{Ba}^{140}\text{-La}^{140}$  WITH INITIAL VOLUME BEFORE ADDITION OF TITRANT EQUAL TO 100.0 ML.

Ml. Titrant	Normalization Factor
0 . . . . .	0.8964
5 . . . . .	0.9249
10 . . . . .	0.9508
15 . . . . .	0.9773
20 . . . . .	1.0000
22.5 . . . . .	1.0085
25 . . . . .	1.0166
27.5 . . . . .	1.0249
30 . . . . .	1.0318
35 . . . . .	1.0446
40 . . . . .	1.0563
50 . . . . .	1.0718

Following titration curves are normalized at 20.0 ml. with respect to the water blank curve in Figure 17.

In each titration the  $\text{Ba}^{140}\text{-La}^{140}$  were present in tracer concentrations in the dish. The solution being titrated was always brought to 100.0 ml. total volume with distilled water



before beginning the titration. In the titration represented by Figure 21 excess  $\text{La}(\text{NO}_3)_3$  was added to the solution in the dish just before beginning the titration. In the titration represented by Figure 22 excess  $\text{NaNO}_3$  was added to the solution in the dish before beginning the titration.

Statistical errors involved in measuring activities from  $\text{Ba}^{140}\text{-La}^{140}$  in the following determinations are represented by the width of the titration curve.

Figure 18 shows the titration curves obtained by precipitating  $\text{AgCNS}$  in the presence of  $\text{Ba}^{140}\text{-La}^{140}$  as  $\text{Ba}^{++}$  and  $\text{La}^{+++}$ .

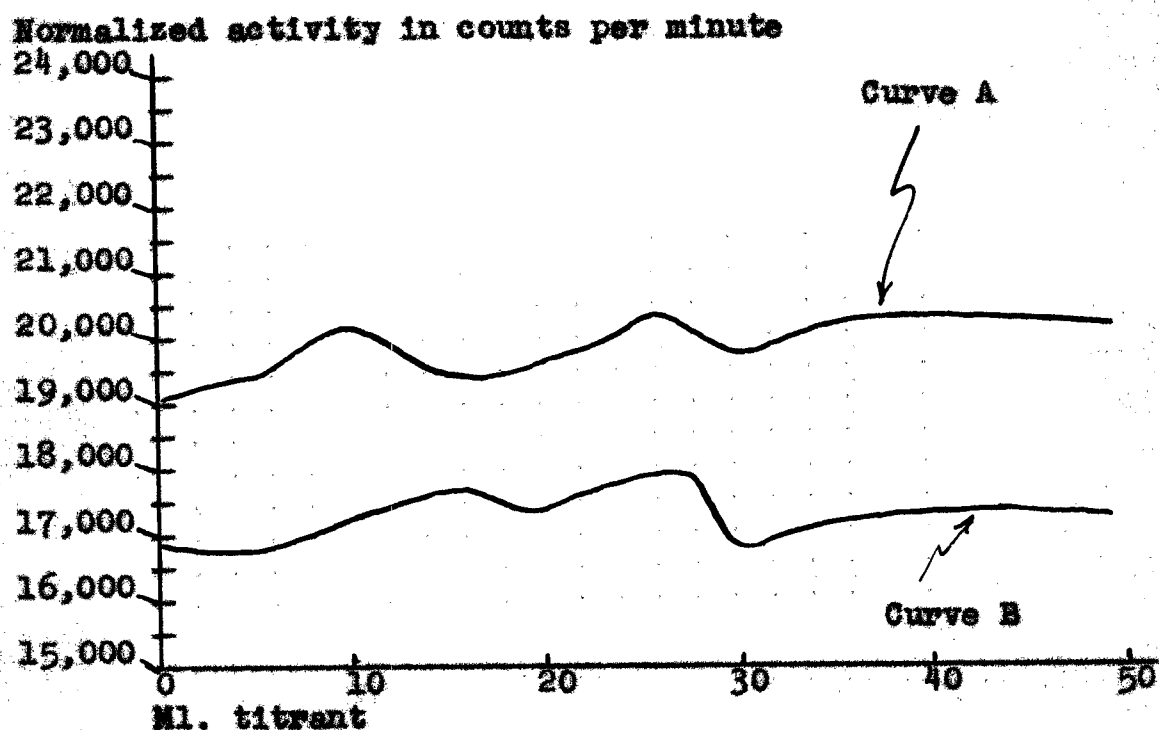


Fig. 18-- $\text{AgCNS}$  in the presence of  $\text{Ba}^{140}\text{-La}^{140}$

Curve A results from adding 0.300 M  $\text{AgNO}_3$  to a solution containing 25.0 ml. of 0.300 M  $\text{NaCNS}$ . Curve B results from

adding 0.300 M NaCNS to a solution containing 25.0 ml. of 0.300 M  $\text{AgNO}_3$ .

Settling of the precipitate was good with very little suspension in solution.

Figure 19 shows the titration curves obtained by precipitating  $\text{AgIO}_3$  in the presence of  $\text{Ba}^{140}\text{-La}^{140}$  as  $\text{Ba}^{++}$  and  $\text{La}^{+++}$ .

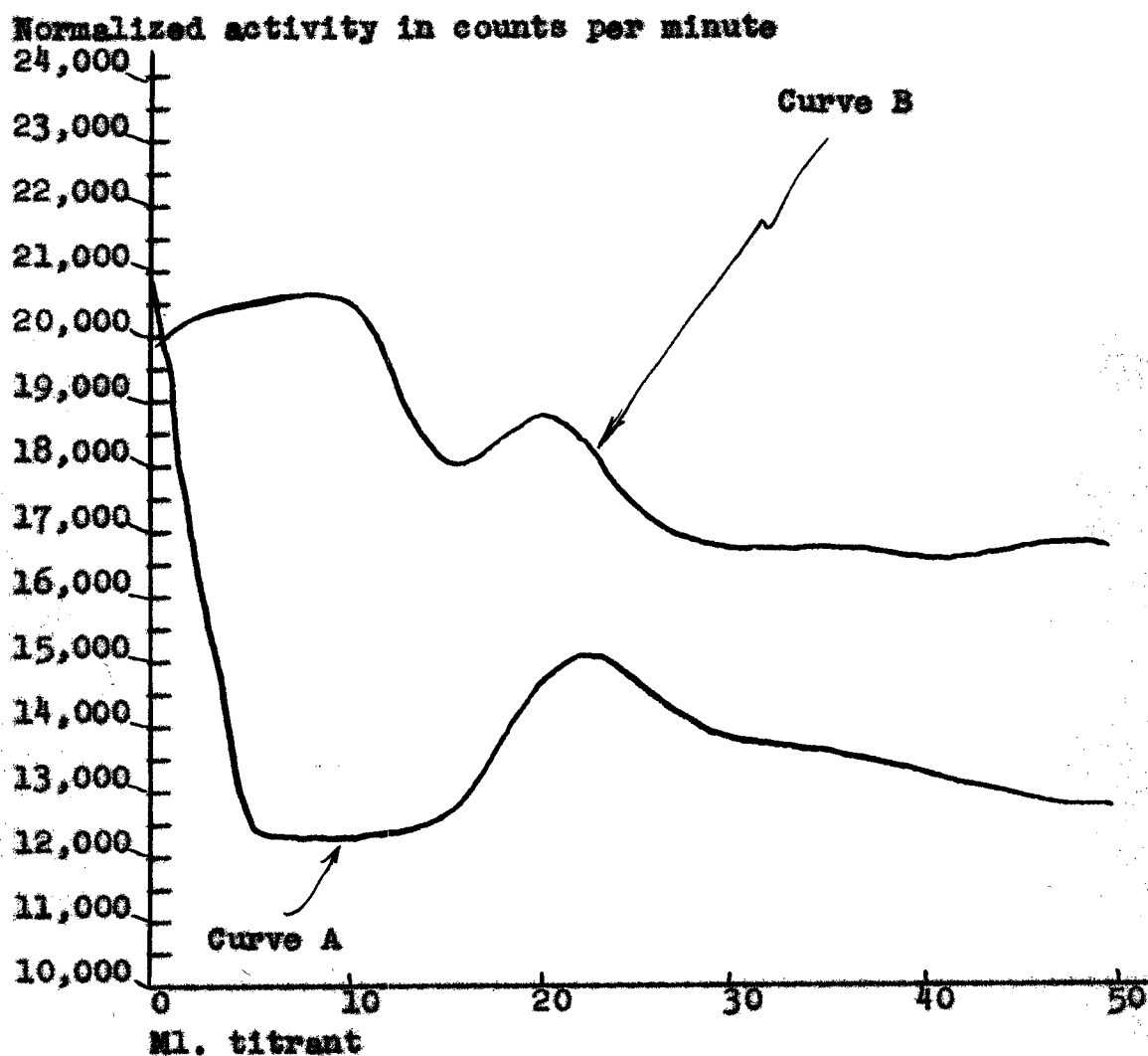


Fig. 19-- $\text{AgIO}_3$  in the presence of  $\text{Ba}^{140}\text{-La}^{140}$

Curve A in Figure 19 results from adding 0.300 M  $\text{AgNO}_3$  to a solution containing 50.0 ml. of 0.150 M  $\text{NaIO}_3$ . Curve B in the same figure results from adding 0.150 M  $\text{NaIO}_3$  to a solution containing 12.50 ml. of 0.300 M  $\text{AgNO}_3$ .

Settling was excellent with no noticeable suspension in solution.

Figure 20 shows the titrations curves obtained by precipitating  $\text{BaSO}_4$  in the presence of  $\text{Ba}^{140}\text{-La}^{140}$  as  $\text{Ba}^{++}$  and  $\text{La}^{+++}$ .

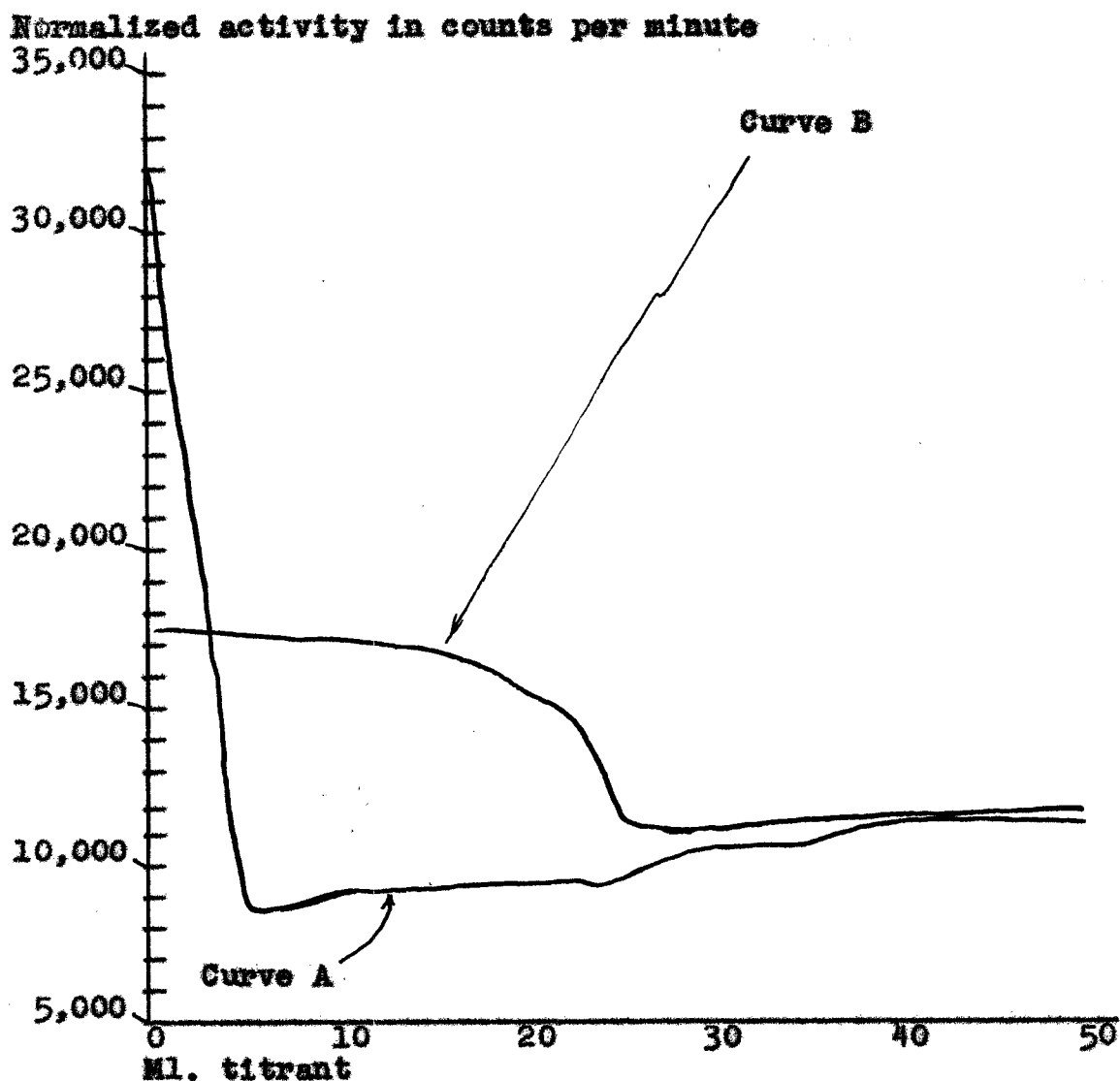


Fig. 20-- $\text{BaSO}_4$  in the presence of  $\text{Ba}^{140}\text{-La}^{140}$

Curve A results from adding 0.100 M  $\text{Ba}(\text{NO}_3)_2$  to a solution containing 25.0 ml. of 0.100 M  $\text{Na}_2\text{SO}_4$ . Curve B results from adding 0.100 M  $\text{Na}_2\text{SO}_4$  to a solution containing 0.100 M  $\text{Ba}(\text{NO}_3)_2$ .

Settling of the precipitate was excellent with very little noticeable suspension in solution.

Figure 21 shows the titration curves obtained by precipitating  $\text{BaSO}_4$  in the presence of  $\text{Ba}^{140}\text{-La}^{140}$  as  $\text{Ba}^{++}$  and  $\text{La}^{+++}$  and excess  $\text{La}(\text{NO}_3)_3$ .

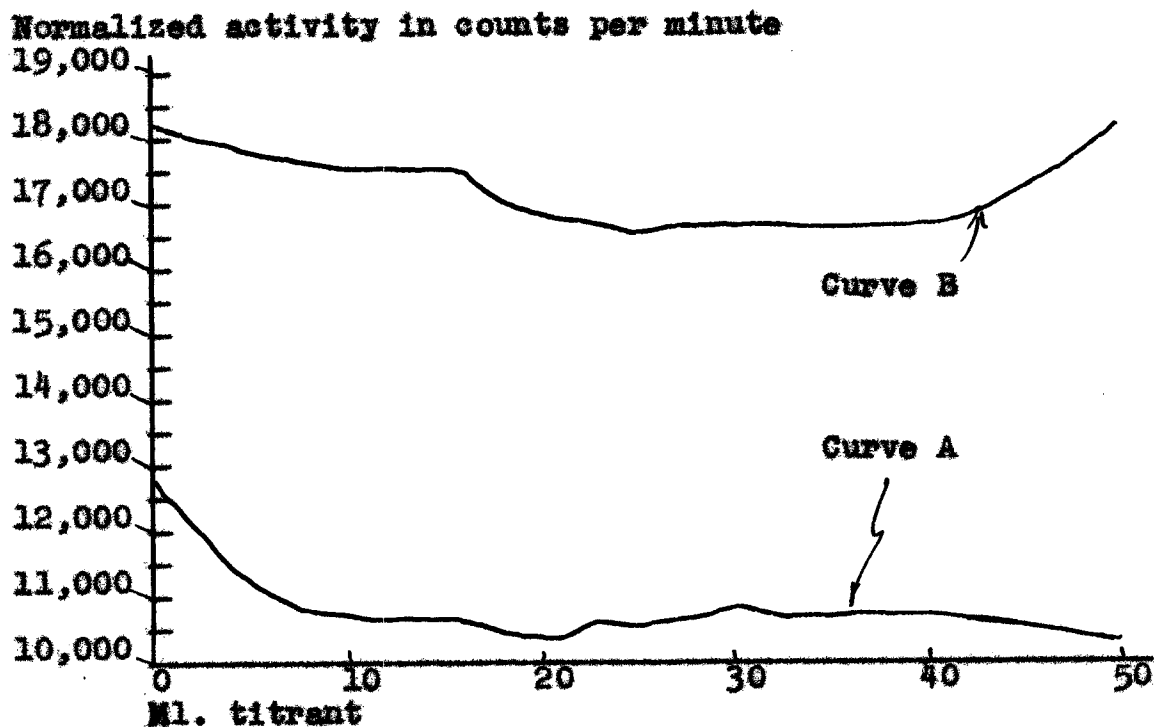


Fig. 21-- $\text{BaSO}_4$  in the presence of  $\text{Ba}^{140}\text{-La}^{140}$  and excess  $\text{La}(\text{NO}_3)_3$  as carrier.

Curve A results from adding 0.100 M  $\text{Ba}(\text{NO}_3)_2$  to a solution containing 25.0 ml. of 0.100 M  $\text{Na}_2\text{SO}_4$  and excess  $\text{La}(\text{NO}_3)_3$ .

Curve B results from adding 0.100 M  $\text{Na}_2\text{SO}_4$  to a solution containing 25.0 ml. of 0.100 M  $\text{Ba}(\text{NO}_3)_2$  in excess  $\text{La}(\text{NO}_3)_3$ .

Figure 22 shows the titration curves obtained by precipitating  $\text{BaSO}_4$  in the presence of  $\text{Ba}^{140}\text{-La}^{140}$  as  $\text{Ba}^{++}$  and  $\text{La}^{+++}$  and excess  $\text{NaNO}_3$ .

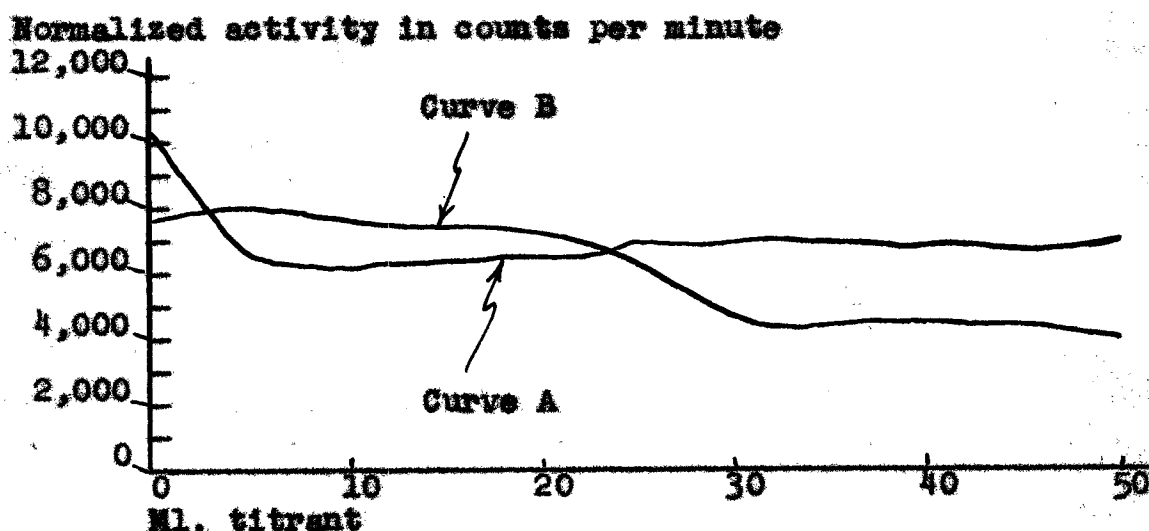


Fig. 22-- $\text{BaSO}_4$  in the presence of  $\text{Ba}^{140}\text{-La}^{140}$  and excess  $\text{NaNO}_3$ .

Curve A results from adding 0.100 M  $\text{Ba}(\text{NO}_3)_2$  to a solution containing 25.0 ml. of 0.100 M  $\text{Na}_2\text{SO}_4$  and excess  $\text{NaNO}_3$ . Curve B results from adding 0.100 M  $\text{Na}_2\text{SO}_4$  to a solution containing 25.0 ml. of 0.100 M  $\text{Ba}(\text{NO}_3)_2$  and excess  $\text{NaNO}_3$ .

Settling of the precipitate was good with little suspension in solution.

#### Investigation with $\text{Ce}^{144}\text{-Pr}^{144}$

The  $\text{Ce}^{144}\text{-Pr}^{144}$  used in this investigation was obtained from the Oak Ridge National Laboratory at \$1.00/mc plus \$10.00

service charge per order. It was produced by fission  $\text{Ce}^{144}$  ( $275d$ )  $\beta \rightarrow \text{Pr}^{144}$  to 98% purity exclusive of  $\text{Ce}^{141}$ . It was carrier-free as  $\text{CeCl}_3$  in less than three normal HCl. The concentration of  $\text{Ce}^{141}$  was less than 10%. This form of  $\text{Ce}^{144}\text{-Pr}^{144}$  is a readily available stock item. Its radiations are listed in Table 9.

TABLE 9  
RADIATIONS FROM  $\text{Ce}^{144}\text{-Pr}^{144}$  IN MEV

Isotope	Radiations	
	Beta	Gamma
$\text{Ce}^{144}$	0.3 0.17	0.13 (strong)
$\text{Pr}^{144}$	3.0 (~90%) 2.3 0.8	2.2 } 1.5 } < (10%) 0.7 }

The half-life of  $\text{Ce}^{144}$  is 275 days, and the half-life of  $\text{Pr}^{144}$  is 17.5 minutes.

The water blank curve for  $\text{Ce}^{144}\text{-Pr}^{144}$  is shown in Figure 23.

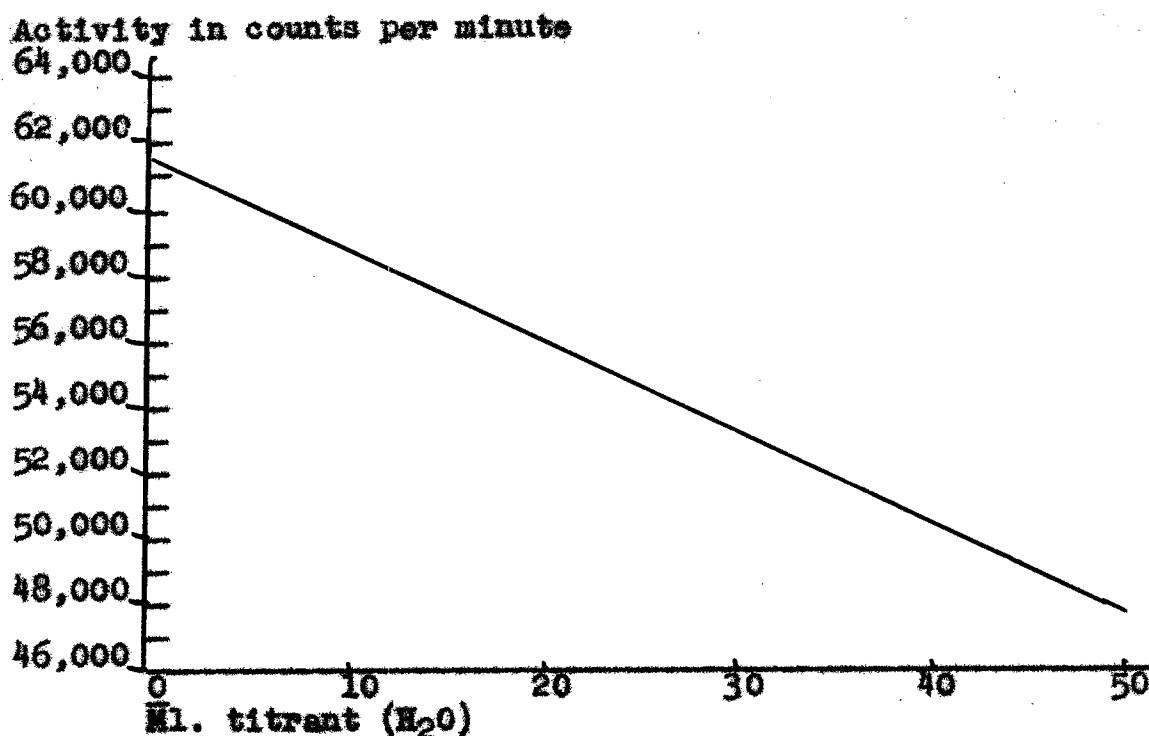


Fig. 23--Water blank curve for Ce<sup>144</sup>-Pr<sup>144</sup>

The normalization factors shown in Table 10 were derived from the water blank curve in Figure 23.

TABLE 10

NORMALIZATION FACTORS FOR Ce<sup>144</sup>-Pr<sup>144</sup> WITH INITIAL VOLUME BEFORE ADDITION OF TITRANT EQUAL TO 100.0 ML.

Ml. Titrant	Normalization Factor
0 . . . . .	0.9104
5 . . . . .	0.9303
10 . . . . .	0.9523
15 . . . . .	0.9764
20 . . . . .	1.0000
22.5 . . . . .	1.0127
25 . . . . .	1.0238
27.5 . . . . .	1.0361
30 . . . . .	1.0507
35 . . . . .	1.0781
40 . . . . .	1.1069
50 . . . . .	1.1707

The following titration curves for  $\text{Ce}^{144}\text{-Pr}^{144}$  as indicator have been normalized at 20.0 ml. titrant with respect to the water blank curve in Figure 23.

In each titration the  $\text{Ce}^{144}\text{-Pr}^{144}$  were present in tracer concentrations in the dish. The solution being titrated was always brought to 100.0 ml. total volume with distilled water before beginning the titration.

Statistical errors involved in measuring activities from the  $\text{Ce}^{144}\text{-Pr}^{144}$  in the following determinations are represented by the width of the titration curves.

Figure 24 shows the titration curves obtained by precipitating  $\text{AgCNS}$  in the presence of  $\text{Ce}^{144}\text{-Pr}^{144}$  as  $\text{Ce}^{+++}$  and  $\text{Pr}^{+++}$ .

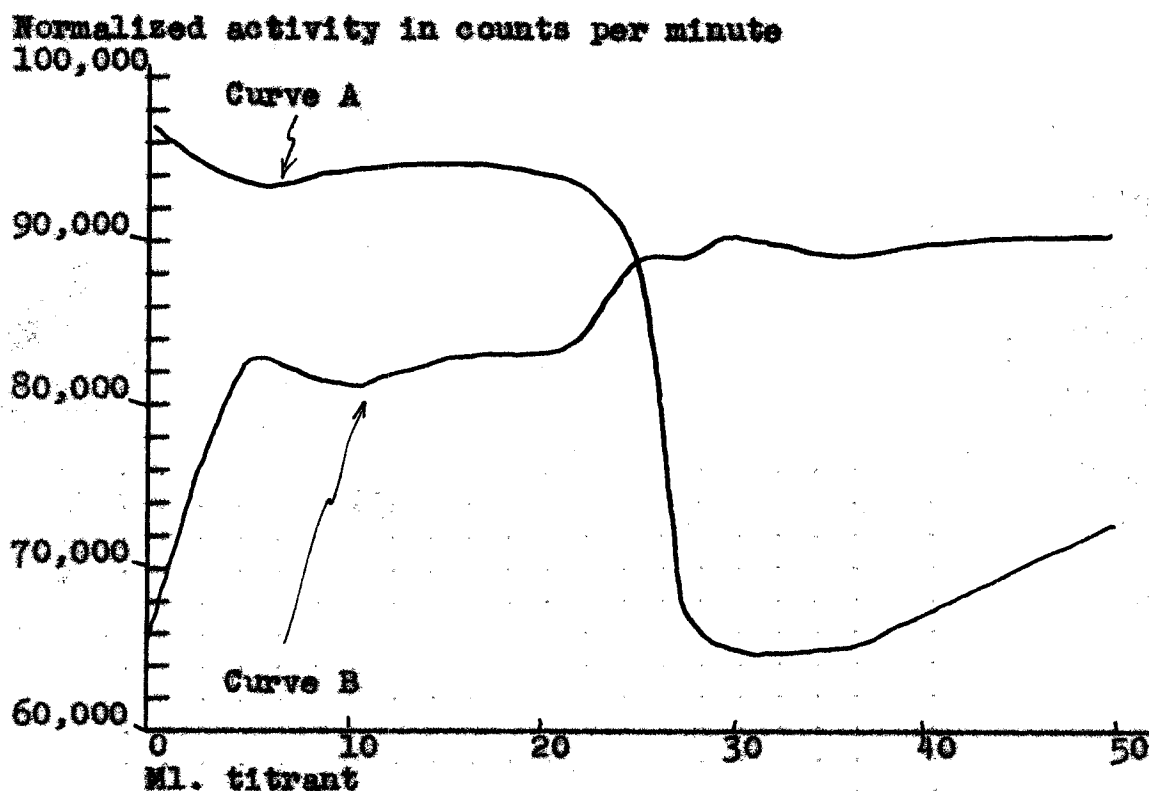


Fig. 24-- $\text{AgCNS}$  in the presence of  $\text{Ce}^{144}\text{-Pr}^{144}$



Curve A results from adding 0.300 M NaCNS to a solution containing 25.0 ml. of 0.300 M  $\text{AgNO}_3$ . Curve B results from adding 0.300 M  $\text{AgNO}_3$  to a solution containing 25.0 ml. of 0.300 M NaCNS.

Settling in both titrations became excellent only after 15.0 ml. titrant. The solutions were turbid up to that point.

Figure 25 shows the titration curves obtained by precipitating  $\text{AgIO}_3$  in the presence of  $\text{Ce}^{144}\text{-Pr}^{144}$  as  $\text{Ce}^{+++}$  and  $\text{Pr}^{+++}$ .

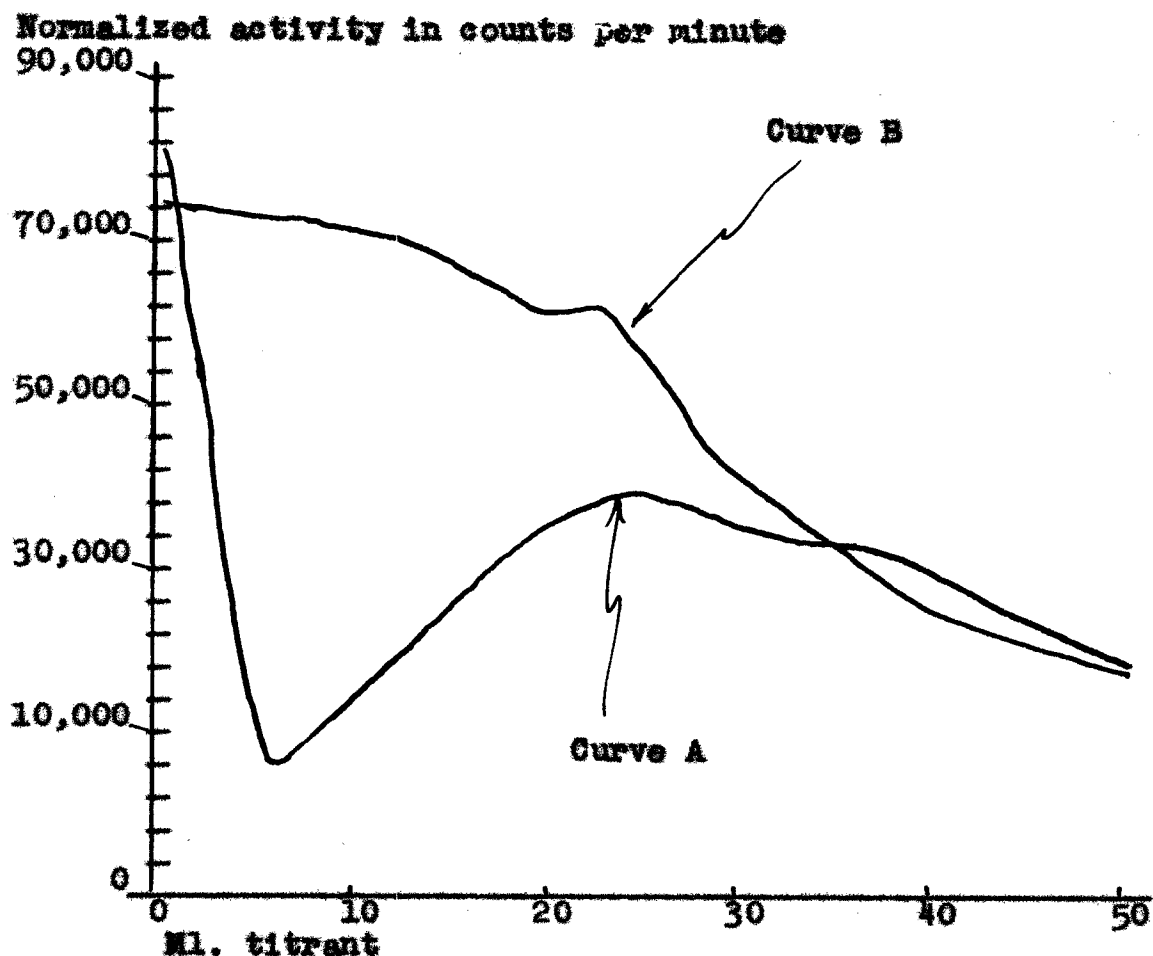


Fig. 25-- $\text{AgIO}_3$  in the presence of  $\text{Ce}^{144}\text{-Pr}^{144}$

Curve A results from adding 0.300 M  $\text{AgNO}_3$  to a solution containing 50.0 ml. of 0.150 M  $\text{NaIO}_3$ . Curve B results from adding 0.150 M  $\text{NaIO}_3$  to a solution containing 12.50 ml. of 0.300 M  $\text{AgNO}_3$ .

Settling was excellent with no noticeable suspension in the solution.

Figure 26 shows the titration curves obtained by precipitating  $\text{BaSO}_4$  in the presence of  $\text{Ce}^{144}\text{-Pr}^{144}$  as  $\text{Ce}^{+++}$  and  $\text{Pr}^{+++}$ .

Normalized activity in counts per minute

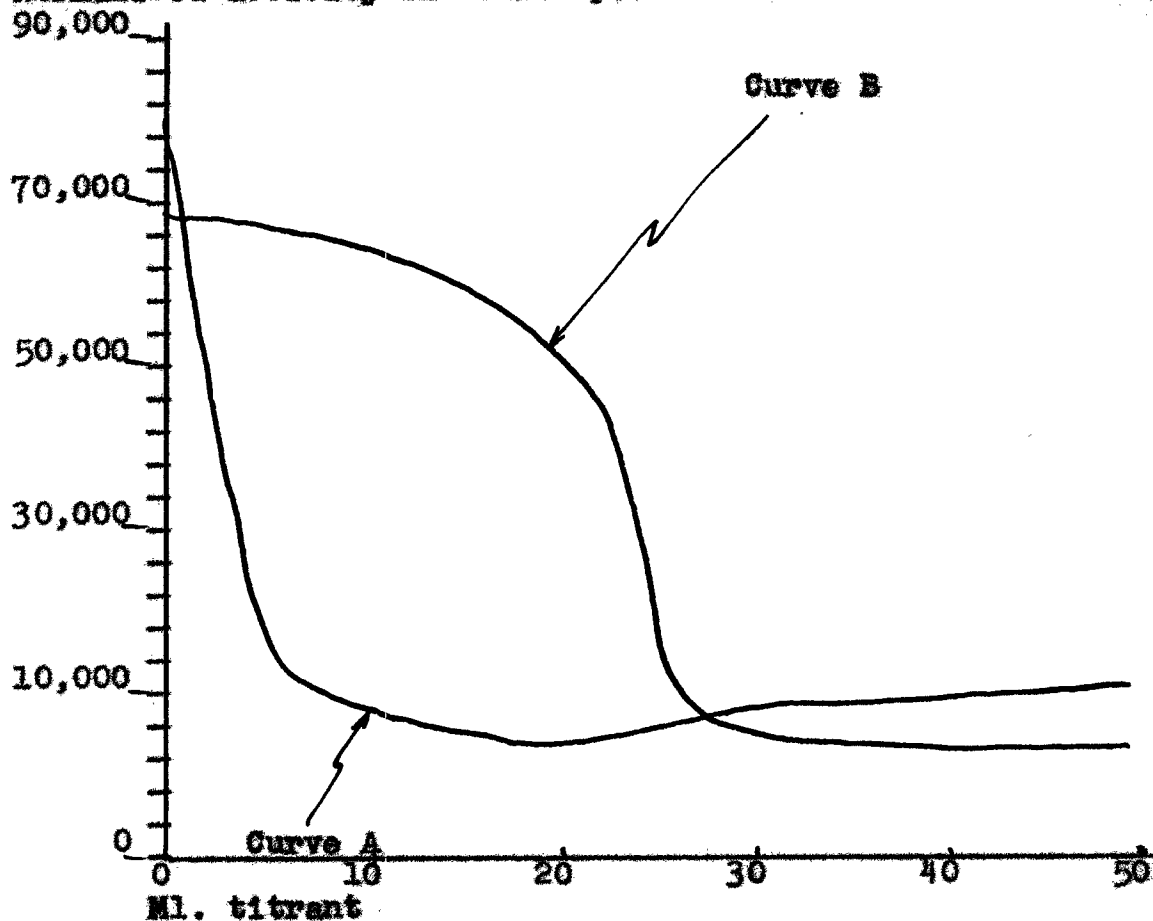


Fig. 26-- $\text{BaSO}_4$  in the presence of  $\text{Ce}^{144}\text{-Pr}^{144}$

Curve A results from adding 0.100 M  $\text{Ba}(\text{NO}_3)_2$  to a solution containing 25.0 ml. of 0.100 M  $\text{Na}_2\text{SO}_4$ . Curve B results from adding 0.100 M  $\text{Na}_2\text{SO}_4$  to a solution containing 25.0 ml. of 0.100 M  $\text{Ba}(\text{NO}_3)_2$ .

Settling was excellent with very little suspension in solution.

Figure 27 shows the titration curves obtained by precipitating  $\text{BaSO}_4$  in the presence of  $\text{Ce}^{144}$ - $\text{Pr}^{144}$  as  $\text{Ce}^{+++}$  and  $\text{Pr}^{+++}$ . This determination is a repetition of the one represented in Figure 26. It was done to check reproducibility.

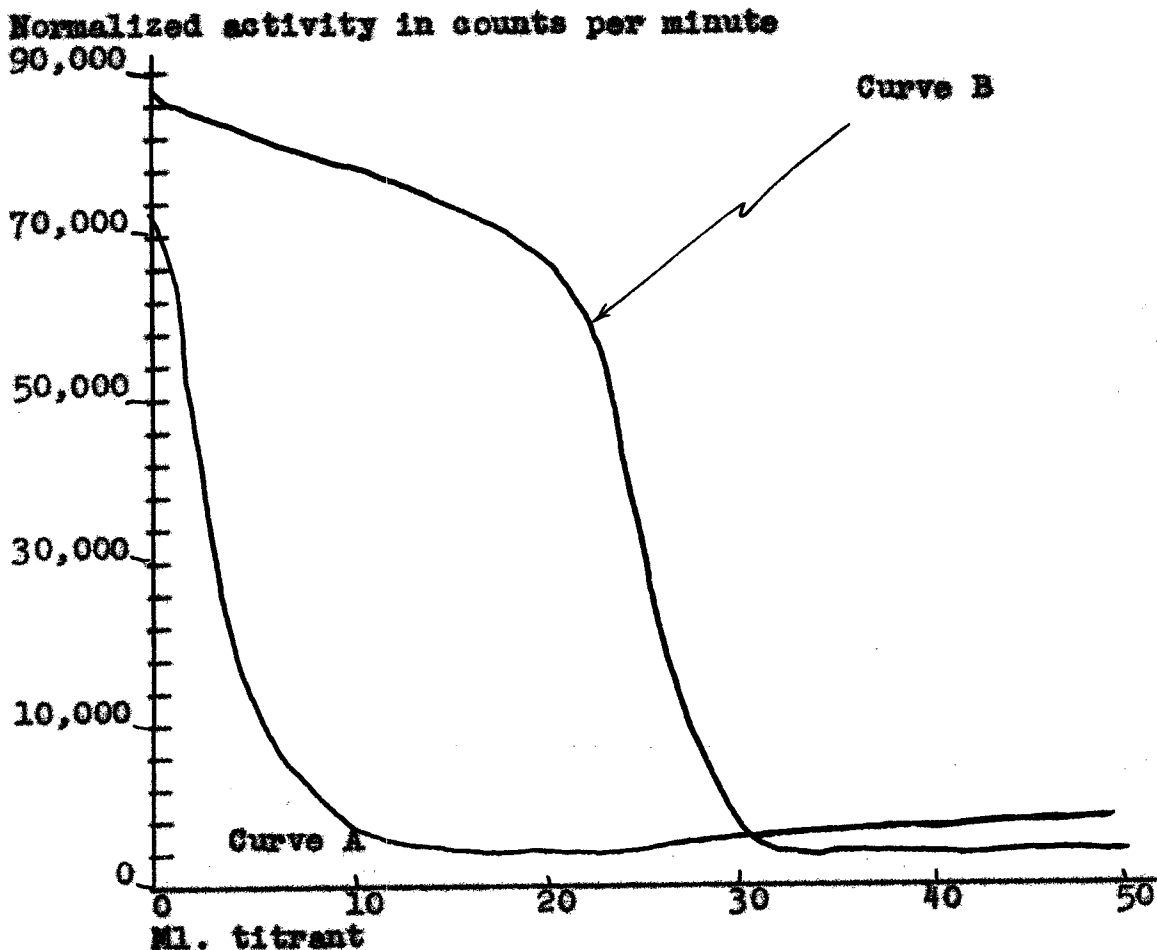


Fig. 27--Repetition of the titration shown in Fig. 26

Curve A results from adding 0.100 M  $\text{Ba}(\text{NO}_3)_2$  to a solution containing 25.0 ml. of 0.100 M  $\text{Na}_2\text{SO}_4$ . Curve B results from adding 0.100 M  $\text{Na}_2\text{SO}_4$  to a solution containing 25.0 ml. of 0.100 M  $\text{Ba}(\text{NO}_3)_2$ .

Settling was excellent with very little suspension in solution.

#### Investigation with Mixed Isotopes

Figure 28 shows the water blank curve obtained using a mixture of  $\text{Ce}^{144}$ - $\text{Pr}^{144}$  and  $\text{P}^{32}$  tracers.

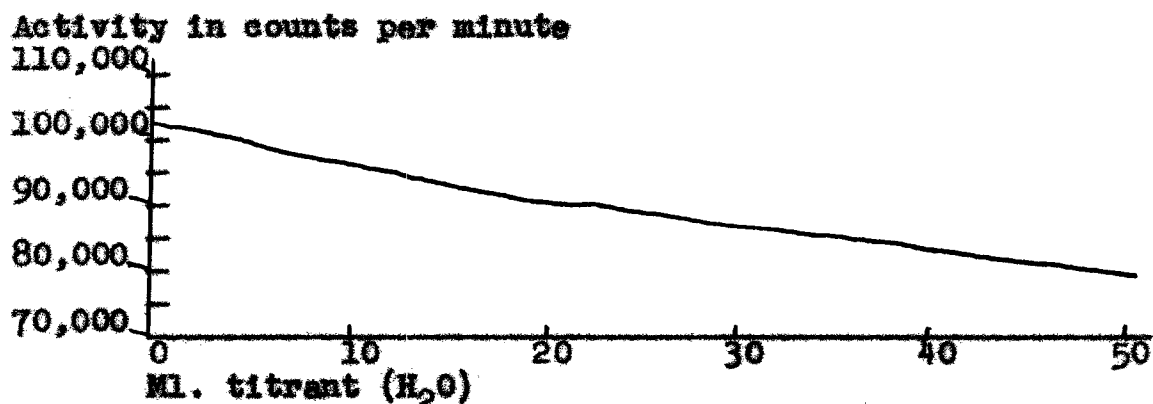


Fig. 28.--Water blank curve for mixture of  $\text{Ce}^{144}$ - $\text{Pr}^{144}$  and  $\text{P}^{32}$  tracers.

The procedure for obtaining the curve in Figure 28 was as follows:

- 1) Put 95.0 ml. distilled water in the dish and take a background count on it; (Background = 130 cpm).
- 2) Add  $\text{P}^{32}$  and take a count for 1.00 minute. (Count = 51,083.)
- 3) Pause 1.00 minute; then add  $\text{Ce}^{144}$ - $\text{Pr}^{144}$ . Take a count for 1.00 minute; (Count = 101,182).

- 4) Bring total volume to 100.0 ml. with  $H_2O$ .
- 5) Begin the titration following the procedure used in preceding titrations.
- 6) After finishing the titration take a background count; (Background = 130 cpm).

The normalization factors in Table 11 were derived from the curve in Figure 28.

TABLE 11

NORMALIZATION FACTORS FOR A MIXTURE OF  $Ce^{144}$ - $Pr^{144}$  AND  $P^{32}$  WITH INITIAL VOLUME BEFORE ADDITION OF TITRANT EQUAL TO 100.0 ML.

ml. Titrant	Normalization Factor
0 . . . . .	0.9010
5 . . . . .	0.9286
10 . . . . .	0.9549
15 . . . . .	0.9785
20 . . . . .	1.0000
22.5 . . . . .	1.0111
25 . . . . .	1.0213
27.5 . . . . .	1.0341
30 . . . . .	1.0436
35 . . . . .	1.0656
40 . . . . .	1.0885
50 . . . . .	1.1375

The following titration curves for the mixture of  $Ce^{144}$ - $Pr^{144}$  and  $P^{32}$  have been normalized at 20.0 ml. titrant with respect to the curve in Figure 28. The solution being titrated was always brought to 100.0 ml. total volume with distilled  $H_2O$ .

Statistical errors are represented by the width of the titration curves.

Figure 29 shows the titration curves obtained by precipitating  $\text{AgCl}$  in the presence of a mixture of  $\text{Ce}^{144}$ - $\text{Pr}^{144}$  and  $\text{P}^{32}$ .

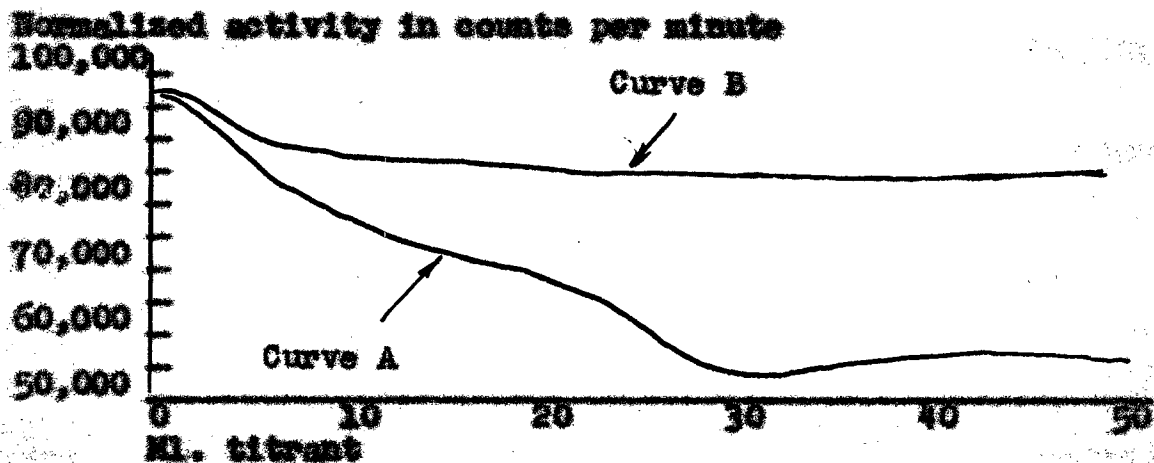


Fig. 29. -- $\text{AgCl}$  in the presence of a mixture of  $\text{Ce}^{144}$ - $\text{Pr}^{144}$  and  $\text{P}^{32}$ .

Curve A results from adding 0.300 M  $\text{NaCl}$  to a solution containing 25.0 ml. of 0.300 M  $\text{AgNO}_3$ . The tracer mixture was obtained by adding  $\text{P}^{32}$  until the activity was 41,202 cpm and then introducing  $\text{Ce}^{144}$ - $\text{Pr}^{144}$  as in the water blank procedure until the activity was 106,590 cpm.

Curve B results from adding 0.300 M  $\text{AgNO}_3$  to a solution containing 25.0 ml. of 0.300 M  $\text{NaCl}$ . The tracer mixture was obtained by adding  $\text{P}^{32}$  until the activity was 42,021 cpm and then introducing  $\text{Ce}^{144}$ - $\text{Pr}^{144}$  as in the water blank procedure until the activity was 107,090 cpm.

Figure 30 shows the titration curve obtained by precipitating  $\text{BaSO}_4$  in the presence of a mixture of  $\text{Ba}^{140}$ - $\text{La}^{140}$  and  $\text{I}^{131}$ .

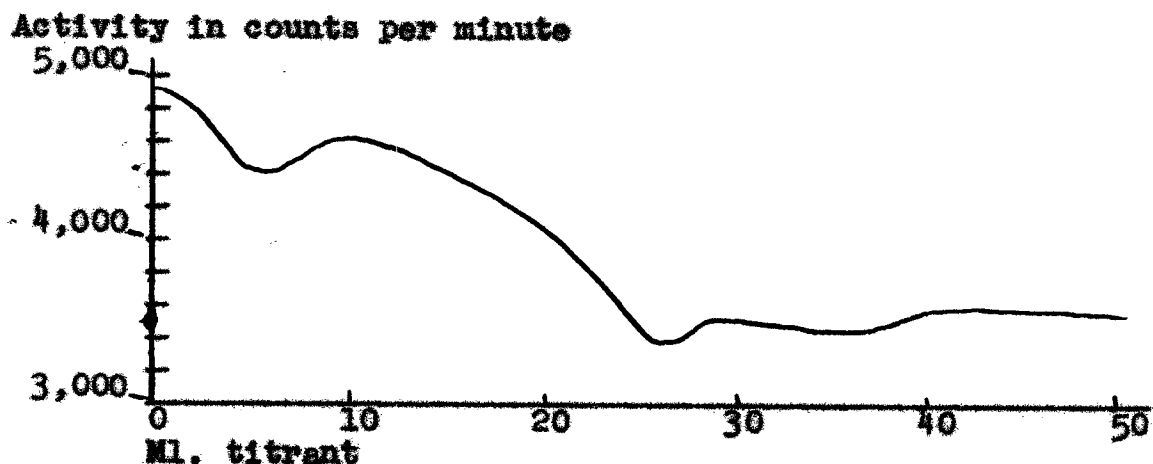


Fig. 30.  $\text{BaSO}_4$  in the presence of a mixture of  $\text{Ba}^{140}$ - $\text{La}^{140}$  and  $\text{I}^{131}$ .

The procedure followed in obtaining Figure 30 was:

- 1) Take a background count (60 cpm).
- 2) Put 25.0 ml. of 0.100 M  $\text{Ba}(\text{NO}_3)_2$  in the dish, add 70 ml.  $\text{H}_2\text{O}$  and  $\text{I}^{131}$ . Record activity (1033 cpm).
- 3) Add  $\text{Ba}^{140}$ - $\text{La}^{140}$  and record activity (5018 cpm).
- 4) Bring total volume to 100.0 ml. with distilled  $\text{H}_2\text{O}$ .
- 5) Begin the titration adding 0.100 M  $\text{Na}_2\text{SO}_4$ .
- 6) After the titration record background (61 cpm).

No water blank was run for the mixture of  $\text{Ba}^{140}$ - $\text{La}^{140}$  and  $\text{I}^{131}$ , as there was only enough  $\text{I}^{131}$  for one determination.

## CHAPTER III

### SUMMARY OF RESULTS

Previous work in this field by Newman P. Bulloch<sup>1</sup> did not yield the same results obtained here. In the previous work a dipping counter tube was used. The active solution was pulled through a filter stick into a cylindrical glass chamber in which the counter tube was placed. The active solution was exposed to a great deal of glass surface. One suggestion made by Mr. Bulloch was that adsorption of the activity on the glass envelope of the counter tube prevented noticeable fluctuations in measured solution activity during the titrations. Another possibility is that the time intervals involved were not held consistent. The apparatus used by Mr. Bulloch was very similar in design to that used by Langer<sup>2</sup> in his radiometric titrations with radioactive phosphorus.

Curve A of Figure 10 in this thesis corresponds to some of Langer's work. He titrated 0.001 M  $\text{Na}_2\text{HPO}_4$  in ammonia and

---

<sup>1</sup>Newman Payne Bulloch, "The Adsorption of Radioactive Isotopes on Precipitates," Unpublished Master's thesis, Dept. of Chemistry, North Texas State College, 1954.

<sup>2</sup>A. Langer, J. Phy. Chem., 45, pp. 639-40.



ammonium chloride solution with 0.01 M  $\text{MgCl}_2$ . The curve obtained by Langer shows the same behavior at the stoichiometric point as curve A of Figure 10 in this thesis. Curve B of Figure 10 is not related to the work of Langer, as he always placed his radiophosphorous in the reagent phosphate solution used in the titration.

### Characteristics of Curves

Several different curve types were observed in this investigation. Two types were prominent in the investigations with  $\text{P}^{32}$ ,  $\text{Ba}^{140}\text{-La}^{140}$ , and  $\text{Ce}^{144}\text{-Pr}^{144}$ . Table 12 lists examples of these two curve types.

TABLE 12  
CURVE TYPES

Type I		Type II	
Figure	Curve	Figure	Curve
7	A	9	B
9	A	11	A
19	A	20	B
20	A	24	A
25	A	25	B
		26	B

Type I curves show rapid adsorption at the beginning of the

titration with noticeable displacement of adsorbed radioactive ions around the stoichiometric point. Type II curves show little adsorption until the stoichiometric point is approached with rapid adsorption around the stoichiometric point and little displacement after it.

The characteristic shape of some of the curves for AgCl is due to floating of the precipitates. The rise in activity during floating shows that activity is concentrated on the precipitate.

The water blank curve for  $I^{131}$  is anomalous to the other water blank curves in this thesis. It is the only water blank curve showing a rise in activity upon dilution of the active solution.  $I^{131}$  is the only tracer in basic solution of NaOH. The  $Na_2SO_3$  preservative added to it insures that the sodium ion concentration will be high compared to the  $I^{131}$  ion concentration. It is possible that the sodium ion acts as a potential determining ion on the surface of the glass dish. The behavior of the activity in curve B, Figure 16 further indicates the necessity of more investigation before an accurate interpretation of the  $I^{131}$  data can be made.

#### Change of Charge Effect

In titrating  $AgNO_3$  with  $NaIO_3$  in the presence of the negatively charged active phosphate ions we get curve A, Figure 2. Curve A in Figure 19 results from titrating  $NaIO_3$  with  $AgNO_3$  in the presence of positively charged active

barium ions. Both curves are similar to each other indicating that the effect of changing the charge of the adsorbed ion is operative. This is further shown by considering the similarity of curve A, Figure 11, curve B, Figure 20, and curve B, Figure 26. Other less prominent similarities also indicate that the effect of changing charge is operative in these determinations.

#### Effect of Addition of Other Materials

Figure 21 results from the precipitation of  $\text{BaSO}_4$  in the presence of  $\text{Ba}^{140}\text{-La}^{140}$  and excess  $\text{La}(\text{NO}_3)_3$ . The  $\text{La}(\text{NO}_3)_3$  was introduced to determine the effect of the presence of a carrier for the  $\text{La}^{140}$  activity. It is apparent that most of the measured activity showing heavy adsorption in Figure 20 comes from adsorbed  $\text{La}^{140}$  ions. This is expected from a consideration of the relative energies of beta emission from  $\text{Ba}^{140}$  and  $\text{La}^{140}$ . The characteristic nature of adsorption of  $\text{Ba}^{140}\text{-La}^{140}$  on  $\text{BaSO}_4$  is destroyed by the addition of carrier.

Figure 22 results from precipitating  $\text{BaSO}_4$  in the presence of  $\text{Ba}^{140}\text{-La}^{140}$  and excess  $\text{NaIO}_3$ . The presence of  $\text{NaIO}_3$  does not destroy the characteristic nature of the adsorption; however, it does not permit adsorption to occur to the extent shown in Figure 20.

Curiosity alone prompted the investigation with mixed isotopes. There seemed to be no improvements on the characteristic nature of adsorption with double activities as indicators.

### Suggestions and Applications

The need for further investigation of  $I^{131}$  determinations introduces a very important question. Perhaps the water blank's behavior is not indicative of the behavior of a dilution in the presence of ions. Perhaps adsorption on the surface of the glass is dependent upon ions in the solution being titrated. Data presented in this thesis may need to be renormalized if this occurs to as great an extent in  $P^{32}$ ,  $Ba^{140}$ - $La^{140}$ , and  $Ce^{144}$ - $Pr^{144}$  determinations as it apparently does in  $I^{131}$  determinations.

In adapting any of these determinations for analytical purposes changes dependent upon the determination must be made. In some curves there occurs a sharp change near the stoichiometric point. However, this change may not be sharp enough to assure great accuracy in analytical determinations. Reproducibility on the more characteristic curves is good as shown by Figures 26 and 27. One possible analytical application might be the volumetric determination of  $BaSO_4$ .

A possible physical application might be made in the study of sedimentation rates. The radiations from active materials adsorbed on the surfaces of sediment particles can be measured with great accuracy.

## BIBLIOGRAPHY

### Books

Bleuler, E., and Goldsmith, G. J., Experimental Nucleonics, New York, Rinehart and Co., Inc., 1952.

Friedlander, G., and Kennedy, J. W., Introduction to Radiochemistry, New York, John Wiley and Sons, Inc., 1949.

Pierce, W. C., and Haenisch, R. L., Quantitative Analysis, Third Edition, New York, John Wiley and Sons, Inc., 1948.

Schweitzer, G. K., and Whitney, I. B., Radioactive Tracer Techniques, New York, D. Van Nostrand, Inc., 1949.

Wahl, A. C., and Bonner, N. A., Radioactivity Applied to Chemistry, New York, John Wiley and Sons, Inc., 1951.

### Periodicals

Impre, L., Phy. Chem., A153, 262-86, 1931.

Langer, A., J. Phys. Chem., 45, 639-43, 1941.

### Unpublished Material

Bullock, Newman Payne, "The Adsorption of Radioactive Isotopes on Precipitates," Unpublished Master's thesis, Department of Chemistry, North Texas State College, 1954, Pp. 27.